

**DIRECT TORQUE CONTROL OF PERMANENT MAGNET  
SYNCHRONOUS MOTOR USING THREE-LEVEL INVERTER**

*Thesis Submitted in the partial fulfilment of the requirements for the award of degree of*

**MASTER OF ENGINEERING  
In  
POWER SYSTEMS & ELECTRIC DRIVES**

*Submitted by:*

**ANITPAL SINGH  
Reg. No: 800841019**

*Under the Supervisions of:*

**Mr. SHAKTI SINGH  
Assistant Professor**

**&**

**Mr. SSSR SARATHBABU DUVVURI**

**Lecturer**



**ELECTRICAL AND INSTRUMENTATION ENGINEERING  
DEPARTMENT**

**THAPAR UNIVERSITY, PATIALA, PUNJAB-147001**

June, 2010

## CERTIFICATE

"I hereby declare that the work which is presented in the thesis report, entitled, "**DIRECT TORQUE CONTROL OF PERMANENT MAGNET SYNCHRONOUS MOTOR USING THREE LEVEL INVERTER**" in partial fulfilment of the requirements for the award of the Master's Degree in Power Systems & Electric Drives, submitted in Electrical and Instrumentation Engineering Department, Thapar University, Patiala, is an authentic record of my initial work carried out under the supervision of Mr. Shakti Singh and Mr. SSSR Sarathbabu Duvvuri, EIED, THAPAR UNIVERSITY, PATIALA."

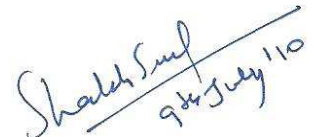
Dated 09.07.2010

  
Anitpal Singh

This is to certify that the above statement made by the candidate is correct and true to the best of our knowledge.

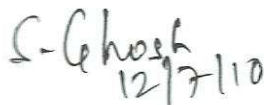
  
7/07/10

**Mr. SSSR Sarathbabu Duvvuri**  
Lecturer, EIED  
Thapar University, Patiala

  
9th July 10

**Mr. Shakti Singh**  
Assistant Professor, EIED  
Thapar University, Patiala

Coutersigned by

  
12/7/10

**Dr. Smarajit Ghosh**  
Professor & Head, EIED  
Thapar University, Patiala

  
25/7

**Dr. R.K. Sharma**  
Dean (Academic Affairs)  
Thapar University, Patiala

## **ACKNOWLEDGMENT**

Working without proper guidance and expecting success is just like making castles in the air, so whenever one wants to start any work, he requires guidance from experts. I express my sincere gratitude to my guide **Mr. Shakti Singh** (Assistant Professor) and **Mr. SSSR Sarathbabu Duvvuri** (Lecturer), Department of Electrical and Instrumentation Engineering, Thapar University, for acting as supervisor and giving valuable guidance during the course of this investigation, for their ever encouraging and timely moral support.

I am greatly thankful to **Dr. Smarajit Ghosh**, Professor and Head, EIED Department, Thapar University for his encouragement and inspiration for execution of the thesis work. I do not find enough words with which I can express my feeling of thanks to entire faculty and staff of Department of Electrical and Instrumentation Engineering, Thapar University, Patiala for their help, inspiration and moral support, which went a long way in successfully completion of my thesis.

I'm grateful to my parents, who involved their own thoughts in my work and gave me worthy suggestions. I'm thankful to all my friends and N Sood for their help during my thesis work.

**Anitpal Singh**

**Reg. No:** 800841019

**Email id:** er\_apsbhamra@yahoo.com

## **ABSTRACT**

Permanent Magnet synchronous motors (PMSMs) are used in many applications that require rapid torque response and high-performance operation. The PMSM is very similar to the standard wound rotor synchronous machine except that the PMSM has no damper windings and excitation is provided by a permanent magnet instead of a field winding. The elimination of field coil, dc supply and slip rings reduce the motor loss and complexity. For the same frame size, permanent magnet motors have higher pull out torque. It is mathematically proven that the increase of electromagnetic torque in a permanent magnet motor is proportional to the increase of the angle between the stator and rotor flux linkages, and, therefore, the fast torque response can be obtained by adjusting the rotating speed of the stator flux linkage as fast as possible. This is achieved by using direct torque control (DTC) technique.

The Direct Torque Control (DTC) has been more and more used in industrial applications with permanent magnet synchronous motor (PMSM) using two level voltage source three-phase inverter with hysteresis controller due to some advantages like: more simplicity, low dependency on the motor parameters, good dynamic torque response. This type of drive system is named as classic PMSM DTC. However, the classic PMSM DTC has some problems like more torque and flux ripples as well as more harmonic contents in the stator current. Hence, to overcome these problems a novel DTC algorithm is proposed for three-phase induction motor which employs a three-level inverter. It is an extension of the classic DTC for two-level inverters. The basic principle of DTC is to directly select stator voltage vectors according to the differences between the references of torque and stator flux linkage and their actual values.

The basic theory of operation for the control technique is presented. A mathematical model for the proposed DTC of the PMSM topology is developed. A simulation model is developed in MATLAB/SIMULINK and is used to verify the basic operation (performance) of the DTC technique.

## List of Figures

	Page no.
2.1 Two pole three phase surface mounted PMSM.	10
3.1 Eight possible voltage space vectors obtained from VSI.	20
3.2 Phasor diagram of a non-salient pole synchronous machine in the Motoring mode.	21
3.3 Incremental stator flux linkage space vector representation in the DQ-plane.	23
3.4 Representation of direct and indirect components of the stator flux linkage vector.	25
3.5 Voltage source inverter (VSI) connected to the R-L load.	26
3.6 Voltage vector selection when the stator flux vector is located in sector $i$ .	28
3.7 Classical DTC scheme.	30
3.8 DTC sectors and reference frames.	32
3.9 VSI vectors used when $\lambda_{dq}$ is in sector 1.	32
3.10 2-level hysteresis comparator.	33
3.11 VSI and how the motor windings are connected.	34
4.1 Three level NPC inverter	39
4.2 Voltage space vectors for a three level NPC inverter	40
4.3 Schematic diagram of the DTC PMSM drive system for Three-level Inverter	42
4.4 Effect of voltage space vectors on torque and stator flux linkages	43
4.5 Voltage unbalancing of the inverter capacitors	44
5.1 Simulink model of PMSM motor	48
5.2 Park's Transformation block	48
5.3 DTC with 2-level inverter	49
5.4 Torque response of DTC with 2-level inverter	50
5.5 Flux trajectory	51

5.6	Stator currents $i_a$ , $i_b$ & $i_c$	51
5.7	Stator flux amplitude waveform	52
5.8	Harmonic spectrum of Stator current	52
5.8	DTC with 3-level inverter	53
5.9	Electro-magnetic torque with 3-level inverter	54
5.10	Flux trajectory in 3-level inverter	54
5.11	Steady state Stator currents $i_a$ , $i_b$ & $i_c$	55
5.12	Stator flux amplitude waveform	55
5.13	Harmonic spectrum of Stator current	56

## LIST OF SYMBOLS

$\lambda_r$	rotor flux
$V_s$	complex space vectors of the three phase stator voltages
$i_s$	currents in the stator winding
$r_s$	resistance of the stator winding
$\lambda_s$	stator flux linkage
$v_{sa}, v_{sb}, v_{sc}$	stator instantaneous phase voltages.
$i_{sa}, i_{sb}, i_{sc}$	stator instantaneous phase currents.
$\lambda_{sa}, \lambda_{sb}, \lambda_{sc}$	stator flux linkages
$L_{aa}, L_{bb}, L_{cc}$	self-inductances of the stator a, b and c-phase respectively.
$L_{ab}, L_{bc}, L_{ca}$	mutual inductances between the a and b phases, b and c phases, and a and c phases, respectively.
$\lambda_{ra}, \lambda_{rb}, \lambda_{rc}$	flux linkages that change depending on the rotor angle established in the stator a, b, and c phase windings
$L_{ls}$	leakage inductance of the stator winding
$L_0$	average inductance
$L_{ms}$	inductance fluctuation
$\theta_r$	angle between the stator D-axis and the rotor d-axis
$f_{abc}$	abc vector
$f_{dq0}$	dq0 vector
$T_{dq0}$	Transformation matrix
$\omega_r$	angular velocity, electrical angle
$v_d$	d-axis voltage
$v_q$	q-axis voltage

$\lambda_d, \lambda_q$	d-axis and q-axis flux linkage
$L_d, L_q$	d-axis and q-axis self inductance
$\lambda_f$	rotor flux amplitude
$R_s$	stator resistance
$T_e$	electro-magnetic Torque
$\omega_m$	angular velocity, mechanical angle
$E$	back emf-constant
$Z_s$	stator impedance
$\delta$	load or torque angle
$P_i, P_o$	input and output power
$P$	number of poles
$L_s$	stator self inductance
$T_s$	sampling time
$V_s$	voltage vector
$V_{1...6}$	voltage vectors 1,2...6
$S_a, S_b, S_c$	state of the switch in each leg a,b and c
$V_{dc}, U_{dc}$	DC bus voltage
$\theta$	sector
$\tau, d\tau$	Torque error
$\psi, d\psi$	flux error
$\psi_s$	stator flux linkage amplitude

## **LIST OF TABLES**

		Page no.
Table 3.1	Switching table	29
Table 3.2	Voltage Vector Switching Table	33
Table 4.1	Switching states of a three level inverter	41
Table 4.2	Voltage space vectors employed in the proposed DTC algorithm	41
Table 4.3	Adopted control strategy	41
Table 5.1	Comparision of PMSM with 2-level and 3-level inverter	56

## **LIST OF ABBREVIATIONS**

VSI	Voltage Source Inverter
PMSM	Permanent Magnet Synchronous Motor
DTC	Direct Torque Control
VC	Vector Control
FOC	Field Oriented Control
DSC	Direct Self Control
THD	Total Harmonic Distortion
AC	Alternating Current
DC	Direct Current
DSP	Digital Signal Processor.
DQ axis	Direct and Quadrature axis
dq axis	direct and quadrature axis
MATLAB	MATrix LABoratory

## Table of Contents

	Page no.
<b>Chapter 1: Introduction</b>	<b>1</b>
1.1 Introduction	2
1.2 Literature Survey	3
1.3 Overview of the Thesis	5
<b>Chapter 2: Mathematical Model of PMSM</b>	<b>6</b>
2.1 Introduction	7
2.2 Permanent Magnet Synchronous Machines	7
2.3 Permanent Magnet Materials	9
2.4 Space Vectors	9
2.5 Park's Transformation	13
2.6 Modeling Equations of PMSM	16
2.7 Summary	17
<b>Chapter 3: Direct Torque Control (DTC) operation OF PMSM Drive</b>	<b>18</b>
3.1 Introduction	19
3.2 Torque control strategy in DTC of PMSM Drive	21
3.3 Flux control strategy in DTC of PMSM Drive	23
3.4 Voltage Vector Selection in DTC of PMSM Drive	25
3.5 Conventional Direct Torque Control System	29
3.5.1 Current Transform	30
3.5.2 Flux Estimator	31
3.5.3 Torque Estimator	31
3.5.4 Sector Calculation	31
3.5.5 Torque and Flux hysteresis comparators	33
3.5.6 Look-up Table	33
3.5.7 Voltage Source Inverter	34

	3.6 Advantages and Disadvantages of Direct Torque Control Technique	35
	3.7 Summary	36
<b>Chapter 4:</b>	<b>Three level Voltage Source Inverter</b>	<b>37</b>
	4.1 Introduction	38
	4.2 Three level Neutral point clamped Inverter	38
	4.3 DTC with a3-level inverter	39
	4.4 Vector selection table for 3-level inverter	40
	4.5 Control algorithm for DC link capacitor voltage unbalancing	44
	4.6 Summary	45
<b>Chapter 5:</b>	<b>Simulation Results</b>	<b>46</b>
	5.1 Introduction	47
	5.2 MATLAB/Simulink model for PMSM	48
	5.3 DTC technique with a 2-level inverter	49
	5.4 DTC technique with a 3-level inverter	53
	5.5 Summary	56
<b>Chapter 6:</b>	<b>Conclusion and Recommendations</b>	<b>57</b>
	<b>Papers from Thesis</b>	<b>59</b>
	<b>References</b>	

# **Chapter 1**

## **Introduction**

# Chapter 1

## 1.1 INTRODUCTION:

Industry automation is mainly developed around motion control systems in which controlled electric motors play a crucial role as heart of the system. Therefore, the high performance motor control systems contribute, to a great extent, to the desirable performance of automated manufacturing sector by enhancing the production rate and the quality of products. In fact the performance of modern automated systems, defined in terms of swiftness, accuracy, smoothness and efficiency, mainly depends to the motor control strategies. The recent developments of the power electronics industry resulted in a considerable increase of the power that can be manipulated by semiconductor devices. In spite of that, the maximum voltage supported by these devices remains the major obstacle in medium and high voltage applications. For such applications multilevel converters have been proposed. Multilevel inverters present lower harmonic distortion of the output voltages when compared to standard two-level inverters operating at the same switching frequency. Newly developed permanent magnet synchronous (PMS) motors with high energy permanent magnet materials particularly provide fast dynamics, efficient operation and very good compatibility with the applications if they are controlled properly. However, the AC motor control including control of PMS motors is a challenging task due to very fast motor dynamics and highly nonlinear models of the machines. Therefore, a major part of motor control development consists of deriving motor mathematical models in suitable forms

There are two competing control strategies for AC motors i.e. vector control (VC) and direct torque control (DTC). Almost 30 years ago, in 1971 F. Blaschke presented the first paper on field-oriented control (FOC) for induction motors. Since that time, the technique was completely developed and today is mature from the industrial point of view. Today field oriented controlled drives are an industrial reality and are available on the market by several producers and with different solutions and performance.

Thirteen years later, a new technique for the torque control of induction motors was developed and presented by I. Takahashi as direct torque control (DTC) and by M. Depenbrock as direct self control (DSC). Since the beginning, the new technique was characterized by simplicity, good performance and robustness. Using DTC or DSC it is possible to obtain a good dynamic control of the torque without any mechanical transducers on the machine shaft. Thus, DTC and DSC can be considered as “sensorless type” control techniques. The basic scheme of DSC is preferable in the high power range applications, where a lower inverter switching frequency can justify higher current distortion.

The name direct torque control is derived by the fact that, on the basis of the errors between the reference and the estimated values of torque and flux, it is possible to directly control the inverter states in order to reduce the torque and flux errors within the prefixed band limits.

Unlike FOC, DTC does not require any current regulator, coordinate transformation and PWM signals. In spite of its simplicity, DTC allows a good torque control in steady-state and transient operating conditions to be obtained. The problem is to quantify how good the torque control is with respect to FOC.

In addition, this controller is very little sensible to the parameters detuning in comparison with FOC.

## **1.2 LITERATURE SURVEY:**

*Direct self control (DSC) of inverter fed induction machine*, this paper proposes a method of simple signal processing which gives three-phase machines fed by VSI an excellent performance even at the low switching frequencies usual in heavy power applications. In DSC the power semiconductors of a three phase VSI are directly switched on and off via three Schmitt triggers, comparing the time integrals of line-to-line voltages to a reference value of desired flux, if the torque has not yet reached an upper limit value of a two-limit torque control. When the upper limit value is reached, zero voltages are switched on to the machine, as long as the lower limit value of torque is not yet under passed.

*Modelling and Simulation of Permanent Magnet Synchronous Motor Drive*, this paper addresses the modeling and simulation of Permanent Magnet Synchronous Motor drive in rotor dq reference frame, it also discusses the Park's Transformation used to transform stator abc quantities to the rotor dq reference frame.

*A Direct Torque Controller for Permanent Magnet Synchronous Motor Drives*, this paper derives the expression of torque production of PMSMs in the stator flux linkage xy-reference frame and finds that the concept of DTC can be also applied in PMSM drive. And also states that the core of DTC, is the control of the amplitude and rotating speed of the stator flux linkage and the calculation of stator flux is then very important. One of the best and simplest calculation methods is to calculate the stator flux from the stator voltage and current, which is independent of the motor parameters except the stator resistance and does not need the coordinate transformation. The switching table for controlling the stator flux for a PMSM is also derived.

*Study on the Direct Torque Control of Permanent Magnet Synchronous Motor Drives*, this paper gives the theoretical basis of the Direct Torque Control (DTC) for Permanent Magnet Synchronous Motor (PMSM). In this paper it is proven that, when the amplitude of the stator flux linkage is kept constant the electromagnetic torque of a PMSM is directly proportional to the sine value of the angle between the flux linkages of the stator and rotor (power angle). Therefore precise torque control can be achieved by controlling the instantaneous speed of the stator flux linkage with its amplitude keeping constant, which is yet fulfilled through the agency of properly selecting the voltage space vector generated by an inverter and its acting time.

*Analysis of Direct Torque Control in Permanent Magnet Synchronous Motor Drives*, in this paper the torque expression in terms of the stator flux linkage and its angle, with respect to the rotor flux linkage, is derived, and then the control of the amplitude and rotating speed of the stator flux linkage are analyzed.

*Direct torque control of permanent magnet synchronous motor drive with a three-level inverter*, this paper proposes that when three level inverter is used in conventional DTC technique, it produces three levels in the phase voltage thus decreasing the phase voltage

harmonic contents without increase the semiconductor devices switching frequency resulting low THD of the motor voltage and current, and also torque and flux ripples reductions when compared with the two-level inverter.

*Research on Direct Torque Control of Permanent Magnet Synchronous Motor Based on Optimized State Selector*, this paper discusses that, in conventional direct torque control (DTC), there are partitioned six sectors in the stationary two-axes reference frame and vectors of stator flux linkage is controlled by selecting different vectors of six voltage vectors. But there are questions in this control method. When stator flux linkage is especially in the adjacent region of two sectors and the amplitude of stator flux linkage is easily fluctuating and more the voltage vector which should be selected is uncertainty. The optimized state selector DTC method is aimed at this ambiguous question. The application of optimized state selector DTC in permanent magnet synchronous motor drivers has the same advantage of conventional DTC, but it has an added advantage in the aspects of decrease of fluctuation of flux linkage and electromagnetic torque, robustness of velocity, as well as decrease of switching power wastage of power devices.

### **1.3 OVERVIEW OF THE THESIS:**

**Chapter 2** gives a detailed theoretical analysis of permanent magnet synchronous motor like construction, advantages and permanent magnet materials used. And also gives the details of modeling of the Permanent Magnet Synchronous Motor.

**Chapter 3** gives the overview of Direct Torque control technique and a methodology is suggested to employ Direct Torque Control technique for a two level inverter driving the PMSM motor.

**Chapter 4** gives the complete description of three level inverter and a control algorithm is developed to avoid voltage unbalance problem in the three level inverter.

**Chapter 5** gives the simulation results of Direct Torque Control technique for a two level inverter and a three level inverter and the results are compared.

**Chapter 6** presents the conclusion and recommendations.

# **Chapter 2**

## **Mathematical Modelling of PMSM**

## **Chapter 2**

### **MATHEMATICAL MODELLING OF PMSM**

#### **2.1 INTRODUCTION:**

Synchronous machines with permanent magnets in the rotor also referred to as PMSMs, have a smaller inertia, higher efficiency and a higher torque to volume ratio compared to asynchronous machines. These advantages have resulted in an increased application of the PMSM in hybrid vehicles, ships, windmills, compressors, pumps and fans. Furthermore high-performance, highly dynamic drives with PMSMs have many applications in such production processes and transport systems where a fast and accurate torque response is required. As reliability and cost of modern PMSM drives are of importance, advanced control techniques have been developed.

In this section, an equivalent two-phase circuit model of a three-phase PM synchronous machine (interior and surface mount) is derived and the concept of the Park's transformation and the relation between three-phase quantities and their equivalent two-phase quantities are also discussed.

#### **2.2 PERMANENT MAGNET SYNCHRONOUS MACHINES:**

Permanent magnet synchronous machines have been widely used in variable speed drives for over a decade now. The most common applications are servo drives in power ranges from a few watts to some kilowatts. A permanent magnet synchronous machine is basically an ordinary AC machine with windings distributed in the stator slots so that the flux created by stator current is approximately sinusoidal and uses permanent magnets to produce the air gap magnetic field rather than using electromagnets. These motors have

significant advantages, attracting the interest of researchers and industry for use in many applications [4].

The popularity of PMSMs comes from their desirable features:

- High efficiency
- High torque to inertia ratio
- High torque to inertia ratio
- High torque to volume ratio
- High air gap flux density
- High power factor
- High acceleration and deceleration rates
- Lower maintenance cost
- Simplicity and ruggedness
- Compact structure
- Linear response in the effective input voltage

However, the higher initial cost, operating temperature limitations, and danger of demagnetization mainly due to the presence of permanent magnets can be restrictive for some applications.

In permanent magnet (PM) synchronous motors, permanent magnets are mounted inside or outside of the rotor. Unlike DC brush motors, permanent magnet synchronous motor requires a “drive” to supply commutated current. This is obtained by pulse width modulation of the DC bus using a DC-to-AC inverter attached to the motor windings. By energizing specific windings in the stator, based on the position of the rotor, a rotating magnetic field is generated. Currents in the stator windings are switched in a predetermined sequence and hence the permanent magnets that provide a constant magnetic field on the rotor follow the rotating stator magnetic field at a constant speed. This speed is dependent on the applied frequency and pole number of the motor. Since the switching frequency is derived from the rotor, the motor cannot lose its synchronism.

The current is always switched before the permanent magnets catch up; therefore the speed of the motor is directly proportional to the current switching rate [2].

Recent developments in the area of semiconductor switches and cost-effective DSPs and microprocessors have opened a new era for the adjustable speed motor drives. Such advances in the motor related sub-areas have helped the field of motor drives by replacing complicated hardware structures with software based control algorithms. The result is considerable improvement in cost while providing better performance of the overall drive system.

### **2.3 PERMANENT MAGNET MATERIALS:**

The properties of the permanent magnet material will affect directly the performance of the motor and proper knowledge is required for the selection of the materials and for understanding PM motors.

The earliest manufactured magnet materials were hardened steel. Magnets made from steel were easily magnetized. However, they could hold very low energy and it was easy to demagnetize. In recent years other magnet materials such as Aluminum Nickel and Cobalt alloys (ALNICO), Strontium Ferrite or Barium Ferrite (Ferrite), Samarium Cobalt (First generation rare earth magnet) (SmCo) and Neodymium Iron-Boron (Second generation rare earth magnet) (NdFeB) have been developed and used for making permanent magnets.

The rare earth magnets are categorized into two classes:

Samarium Cobalt (SmCo) magnets and Neodymium Iron Boride (NdFeB) magnets. SmCo magnets have higher flux density levels but they are very expensive. NdFeB magnets are the most common rare earth magnets used in motors these days [2].

### **2.4 SPACE VECTORS:**

In a permanent magnet synchronous motor (PMSM) where the inductances vary as a function of the rotor angle, the two-phase (d-q) equivalent circuit model is a perfect solution to analyze the multiphase machines because of its simplicity and intuition [3].

Conventionally, a two-phase equivalent circuit model instead of complex three-phase model has been used to analyze reluctance synchronous machines. This theory is now applied in the analysis of other types of motors including PM synchronous motors, induction motors etc.

Comparing a primitive version of a PMSM with wound-rotor synchronous motor, the stator of a PMSM has windings similar to those of the conventional wound-rotor synchronous motor which is generally three-phase, Y-connected, and sinusoidally distributed. However, on the rotor side instead of the electrical-circuit seen in the wound-rotor synchronous motor, constant rotor flux ( $\lambda_r$ ) provided by the permanent magnet in/on the rotor should be considered in the d-q model of a PMSM.

The space vector form of the stator voltage equation in the stationary reference frame is given as:

$$v_s = r_s i_s + d\lambda_s/dt \quad (2.1)$$

where  $r_s$ ,  $V_s$ ,  $i_s$ , and  $\lambda_s$  are the resistance of the stator winding, complex space vectors of the three phase stator voltages, currents, and flux linkages, all expressed in the stationary reference frame fixed to the stator, respectively.

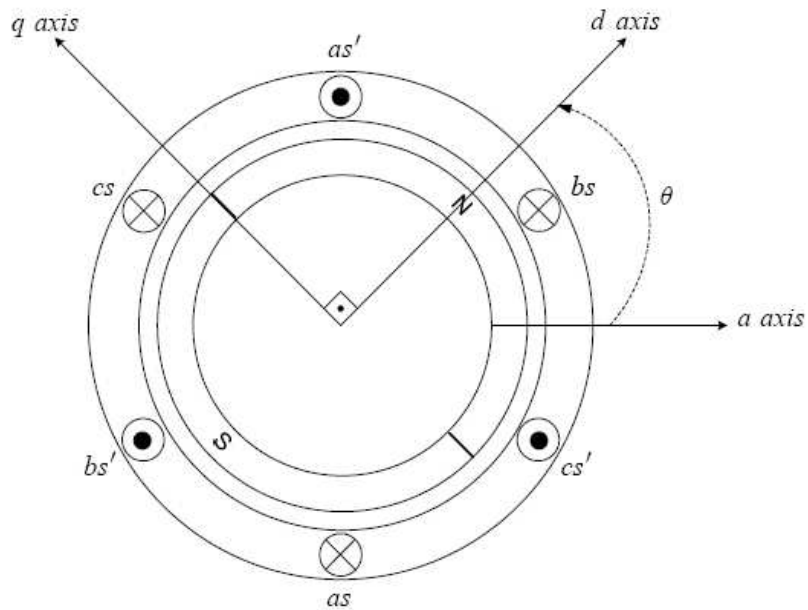


Figure 2.1. Two pole three phase surface mounted PMSM [4].

They are defined as:

$$\begin{aligned}
 v_s &= \frac{2}{3} [v_{sa}(t) + av_{sb}(t) + a^2v_{sc}(t)] \\
 i_s &= \frac{2}{3} [i_{sa}(t) + ai_{sb}(t) + a^2i_{sc}(t)] \\
 \lambda_s &= \frac{2}{3} [\lambda_{sa}(t) + a\lambda_{sb}(t) + a^2\lambda_{sc}(t)]
 \end{aligned} \tag{2.2}$$

Fig. 2.1 illustrates a conceptual cross-sectional view of a three-phase, two-pole surface PM synchronous motor along with the two-phase d-q rotating reference frame.

Symbols used in (2.2) are explained in detail below:

$a$ , and  $a^2$  are spatial operators for orientation of the stator windings;

$$a = e^{j2\pi/3} \quad \text{and} \quad a^2 = e^{j4\pi/3}$$

$v_{sa}$ ,  $v_{sb}$ ,  $v_{sc}$  are the values of stator instantaneous phase voltages.

$i_{sa}$ ,  $i_{sb}$ ,  $i_{sc}$  are the values of stator instantaneous phase currents.

$\lambda_{sa}$ ,  $\lambda_{sb}$ ,  $\lambda_{sc}$  are the stator flux linkages and are given by:

$$\begin{aligned}
 \lambda_{sa} &= L_{aa}i_a + L_{ab}i_b + L_{ac}i_c + \lambda_{ra} \\
 \lambda_{sb} &= L_{ab}i_a + L_{bb}i_b + L_{bc}i_c + \lambda_{rb} \\
 \lambda_{sc} &= L_{ac}i_a + L_{bc}i_b + L_{cc}i_c + \lambda_{rc}
 \end{aligned} \tag{2.3}$$

where

$L_{aa}$ ,  $L_{bb}$ , and  $L_{cc}$ , and are the self-inductances of the stator a-phase, b-phase, and c-phase respectively.

$L_{ab}$ ,  $L_{bc}$  and  $L_{ca}$ , are the mutual inductances between the a- and b-phases, b- and c-phases, and a- and c-phases, respectively.

$\lambda_{ra}$ ,  $\lambda_{rb}$  and  $\lambda_{rc}$  are the flux linkages that change depending on the rotor angle established in the stator a, b, and c phase windings, respectively, due to the presence of the permanent magnet on the rotor.

They are expressed as:

$$\begin{aligned}
\lambda_{ra} &= \lambda_r \cos\theta \\
\lambda_{rb} &= \lambda_r \cos(\theta - 120^\circ) \\
\lambda_{rc} &= \lambda_r \cos(\theta + 120^\circ)
\end{aligned} \tag{2.4}$$

In (2.4),  $\lambda_r$  represents the peak flux linkage due to the permanent magnet. It is often referred to as the back-EMF constant.

Note that in the flux linkage equations, inductances are the functions of the rotor angle, Self-inductance of the stator a-phase winding,  $L_{aa}$  including leakage inductance and a- and b-phase mutual inductance,  $L_{ab} = L_{bc}$  have the form:

$$\begin{aligned}
L_{aa} &= L_{ls} + L_0 - L_{ms} \cos(2\theta) \\
L_{ab} = L_{ba} &= \frac{1}{2} L_0 - L_{ms} \cos\left(2\theta - \frac{2\pi}{3}\right)
\end{aligned} \tag{2.5}$$

where  $L_{ls}$  is the leakage inductance of the stator winding due to the armature leakage flux.  $L_0$  is the average inductance; due to the space fundamental air-gap flux;

$$L_0 = \frac{1}{2} (L_q + L_d)$$

$L_{ms}$  is the inductance fluctuation (saliency); due to the rotor position dependent on flux;

$$L_{ms} = \frac{1}{2} (L_d - L_q)$$

Similar to that of  $L_{aa}$  but with  $\theta$  replaced by  $(\theta - 2\pi/3)$  and  $(\theta - 4\pi/3)$  b-phase and c-phase self-inductances,  $L_{bb}$  and  $L_{cc}$ , can also be obtained, respectively.

All stator inductances are represented in matrix form below:

$$L_{ss} = \begin{bmatrix} L_{ls} + L_0 - L_{ms} \cos 2\theta & -\frac{1}{2} L_0 - L_{ms} \cos 2\left(\theta - \frac{\pi}{3}\right) & -\frac{1}{2} L_0 - L_{ms} \cos 2\left(\theta + \frac{\pi}{3}\right) \\ -\frac{1}{2} L_0 - L_{ms} \cos 2\left(\theta - \frac{\pi}{3}\right) & L_{ls} + L_0 - L_{ms} \cos 2\left(\theta - \frac{2\pi}{3}\right) & -\frac{1}{2} L_0 - L_{ms} \cos 2(\theta - \pi) \\ -\frac{1}{2} L_0 - L_{ms} \cos 2\left(\theta + \frac{\pi}{3}\right) & -\frac{1}{2} L_0 - L_{ms} \cos 2(\theta + \pi) & L_{ls} + L_0 - L_{ms} \cos 2\left(\theta + \frac{2\pi}{3}\right) \end{bmatrix} \tag{2.6}$$

It is evident from the above equation that the elements of  $L_{ss}$  are a function of the rotor angle which varies with time at the rate of the speed of rotation of the rotor.

Under a three-phase balanced system with no rotor damping circuit and knowing the flux linkages, stator currents, and resistances of the motor, the electrical three-phase dynamic equation in terms of phase variables can be arranged in matrix form similar to that of (2.1) written as:

$$[v_s] = [r_s] [i_s] + d/dt [\lambda_s] \quad (2.7)$$

where,

$$\begin{aligned} [v_s] &= [v_{sa}, v_{sb}, v_{sc}]^t \\ [i_s] &= [i_{sa}, i_{sb}, i_{sc}]^t \\ [r_s] &= [r_a, r_b, r_c]^t \\ [\lambda_s] &= [\lambda_{sa}, \lambda_{sb}, \lambda_{sc}]^t \end{aligned} \quad (2.8)$$

In (2.7),  $[v_s]$ ,  $[i_s]$ , and  $[\lambda_s]$  refer to the three-phase applied voltages, three-phase stator currents, and three-phase stator flux linkages in matrix forms as shown in (2.8), respectively. Furthermore,  $[r_s]$  is the diagonal matrix in which under balanced three-phase conditions, all phase resistances are equal to each other and represented as a constant,  $r_s = r_a = r_b = r_c$ , not in matrix form.

## 2.5 PARK'S TRANSFORMATION:

As it was discussed before,  $L_{ss}$  has time-dependent coefficients which present computational difficulty when (2.1) is being used to solve for the phase quantities directly. To obtain the phase currents from the flux linkages, the inverse of the time-varying inductance matrix will have to be computed at every time step. The computation of the inverse at every time step is time-consuming and could produce numerical stability problems. To remove the time-varying quantities in voltages, currents, flux linkages and phase inductances, stator quantities are transformed to a d-q rotating reference frame.

This results in the voltages, currents, flux linkages, part of the flux linkages equation and inductance equations having time-invariant coefficients. In the idealized machine, the rotor windings are already along the d- and q-axes, only the stator winding quantities need transformation from three-phase quantities to the two-phase d-q rotor rotating reference frame quantities. To do so, Park's Transformation is used to transform the stator quantities of an AC machine onto a d-q reference frame that is fixed to the rotor, with the positive d-axis aligned with the magnetic axis of the rotor which has a permanent magnet in PMSMs. The positive q-axis is defined as leading the positive d-axis by  $\pi/2$  in the original Park's Transformation, as shown in Fig. 2.1 [4].

The original Park's Transformation equation is of the form:

$$[f_{dq0}] = [T_{dq0}(\theta_r)][f_{abc}] \quad (2.9)$$

where the d-q transformation matrix is defined as:

$$[T_{dq0}(\theta_r)] = \frac{2}{3} \begin{pmatrix} \cos\theta_r & \cos(\theta_r - \frac{2\pi}{3}) & \cos(\theta_r + \frac{2\pi}{3}) \\ -\sin\theta_r & -\sin(\theta_r - \frac{2\pi}{3}) & -\sin(\theta_r + \frac{2\pi}{3}) \\ \frac{1}{2} & \frac{1}{2} & \frac{1}{2} \end{pmatrix} \quad (2.10)$$

and its inverse is given by

$$[T_{dq0}(\theta_r)]^{-1} = \begin{pmatrix} \cos\theta_r & -\sin\theta_r & 1 \\ \cos(\theta_r - \frac{2\pi}{3}) & -\sin(\theta_r - \frac{2\pi}{3}) & 1 \\ \cos(\theta_r + \frac{2\pi}{3}) & -\sin(\theta_r + \frac{2\pi}{3}) & 1 \end{pmatrix} \quad (2.11)$$

The original d-q Park's Transformation  $[T_{dq0}(\theta_r)]$  is applied to the stator quantities shown in (2.7). This is given by:

$$\begin{aligned} [v_{dq0}] &= [T_{dq0}(\theta_r)][v_s] \\ [i_{dq0}] &= [T_{dq0}(\theta_r)][i_s] \\ [\lambda_{dq0}] &= [T_{dq0}(\theta_r)][\lambda_s] \end{aligned} \quad (2.12)$$

where

$$[v_{dq0}] = [v_d v_q v_0] \quad (2.13)$$

When the three-phase system is symmetrical and the voltages form a balanced three-phase set of  $abc$  sequences, the sum of the set is zero, hence the third components of the d-q quantities in (2.13) are zero, e.g.  $v_0 = 0$ .

If (2.12) is substituted into (2.7), then the stator voltage equation is written in d-q coordinates as:

$$[v_{dq0}] = [T_{dq0}(\theta_r)][r_s][T_{dq0}(\theta_r)]^{-1}[i_{dq0}] + [T_{dq0}(\theta_r)]p[T_{dq0}(\theta_r)]^{-1}[\lambda_{dq0}] \quad (2.14)$$

where,  $p$  is the differential operation

In a three-phase balanced system, all  $p = \frac{d}{dt}$  the phase resistances are equal,  $r_a = r_b = r_c = r_s$ , such that the resistive drop term in the above equation reduces to

$$[T_{dq0}(\theta_r)][r_s][T_{dq0}(\theta_r)]^{-1}[i_{dq0}] = r_s[i_{dq0}] \quad (2.15)$$

The second term having a derivative part in (2.14) can be manipulated and is given by:

$$[T_{dq0}(\theta_r)](p[T_{dq0}(\theta_r)]^{-1}) = \omega \begin{pmatrix} 0 & -1 & 0 \\ 1 & 0 & 0 \\ 0 & 0 & 0 \end{pmatrix} \quad (2.16)$$

Equations (2.15) and (2.16) yield the following result, written in expanded matrix form:

$$\begin{bmatrix} v_d \\ v_q \\ v_0 \end{bmatrix} = r_s \begin{bmatrix} i_d \\ i_q \\ i_0 \end{bmatrix} + \omega_r \begin{pmatrix} 0 & -1 & 0 \\ 1 & 0 & 0 \\ 0 & 0 & 0 \end{pmatrix} \begin{bmatrix} \lambda_d \\ \lambda_q \\ \lambda_0 \end{bmatrix} + p \begin{bmatrix} \lambda_d \\ \lambda_q \\ \lambda_0 \end{bmatrix} \quad (2.17)$$

The transformed motor equations from the three phase stator reference frame to two phase rotating rotor reference frame is given above.

## 2.6 MODELLING OF PMSM:

The model of PMSM without damper winding has been developed on rotor reference frame using the following assumptions [2]:

- 1) Saturation is neglected.
- 2) The induced EMF is sinusoidal.
- 3) Eddy currents and hysteresis losses are negligible.
- 4) There are no field current dynamics.

Voltage equations are given by:

$$\begin{aligned} v_d &= R_s i_d - \omega_r \lambda_q + \frac{d\lambda_d}{dt} \\ v_q &= R_s i_q - \omega_r \lambda_d + \frac{d\lambda_q}{dt} \end{aligned} \quad (2.18)$$

Flux Linkages are given by

$$\begin{aligned} \lambda_d &= L_d i_d + \lambda_f \\ \lambda_q &= L_q i_q \end{aligned} \quad (2.19)$$

Substituting equations 2.19 in 2.18:

$$\begin{aligned} v_d &= R_s i_d - \omega_r L_q i_q + \frac{d}{dt} (L_d i_d + \lambda_f) \\ v_q &= R_s i_q - \omega_r L_d i_d + \frac{d}{dt} (L_q i_q) \end{aligned} \quad (2.20)$$

Arranging equations 2.20 in matrix form

$$\begin{pmatrix} v_d \\ v_q \end{pmatrix} = \begin{pmatrix} R_s + sL_d & -\omega_r L_q \\ \omega_r L_d & R_s + sL_q \end{pmatrix} \begin{pmatrix} i_d \\ i_q \end{pmatrix} + \begin{pmatrix} 0 \\ \omega_r \lambda_f \end{pmatrix} \quad (2.21)$$

The developed torque motor is being given by

$$T_e = \frac{3}{2} \left( \frac{P}{2} \right) (\lambda_d i_q - \lambda_q i_d) \quad (2.22)$$

The mechanical Torque equation is

$$T_e = T_L + B\omega_m + J \frac{d\omega_m}{dt} \quad (2.23)$$

Solving for the rotor mechanical speed from equation 2.23,

$$\omega_m = \int \left( \frac{T_e - T_L - B\omega_m}{J} \right) dt \quad (2.24)$$

and  $\omega_m = \omega_r \left( \frac{2}{P} \right)$

In the above equations  $\omega_r$  is the rotor electrical speed where as  $\omega_m$  is the rotor mechanical speed.

## 2.7 SUMMARY:

This chapter presents a theoretical review of permanent magnet motors drives which includes permanent magnet materials, classification of the permanent magnet motors, the construction and advantages. And also deals with the detailed modeling of a permanent magnet synchronous motor and derives equivalent two phase mathematical model of the permanent magnet synchronous motor which can be easily implemented in MATLAB/Simulink.

# **Chapter 3**

## **Direct Torque Control (DTC) of PMSM Drive**

## Chapter 3

### DIRECT TORQUE CONTROL (DTC) OF PMSM DRIVE

#### 3.1 INTRODUCTION:

Today there are basically two types of instantaneous electromagnetic torque-controlled AC drives used for high-performance applications: vector and direct torque control (DTC) drives. The most popular method, vector control was introduced more than 25 years ago in Germany by Hasse, Blaske and Leonhard. The vector control method, also called Field Oriented Control (FOC) transforms the motor equations into a coordinate system that rotates in synchronism with the rotor flux vector. Under a constant rotor flux amplitude there is a linear relationship between the control variables and the torque. Transforming the AC motor equations into field coordinates makes the FOC method resemble the decoupled torque production in a separately excited DC motor. Over the years, FOC drives have achieved a high degree of maturity in a wide range of applications. They have established a substantial world wide market which continues to increase.

When there was still a trend toward standardization of control systems based on the FOC method, direct torque control was introduced in Japan by Takahashi and Nagochi and also in Germany by Depenbrock. Their innovative studies depart from the idea of coordinate transformation and the analogy with DC motor control. These innovators proposed a method that relies on a bang-bang control instead of a decoupling control which is the characteristic of vector control. Their technique (bang-bang control) works very well with the on-off operation of inverter semiconductor power devices.

After the innovation of the DTC method it has gained much momentum. The basic concept behind the DTC of AC drive, as its name implies, is to control the electromagnetic torque and flux linkage directly and independently by the use of six or eight voltage space vectors found in lookup tables. The possible eight voltage space vectors used in DTC are shown in Fig. 3.1[7]-[9].

The typical DTC includes two hysteresis controllers, one for torque error correction and one for flux linkage error correction. The hysteresis flux controller makes the stator flux rotate in a circular fashion along the reference trajectory. The hysteresis torque controller tries to keep the motor torque within a pre-defined hysteresis band.

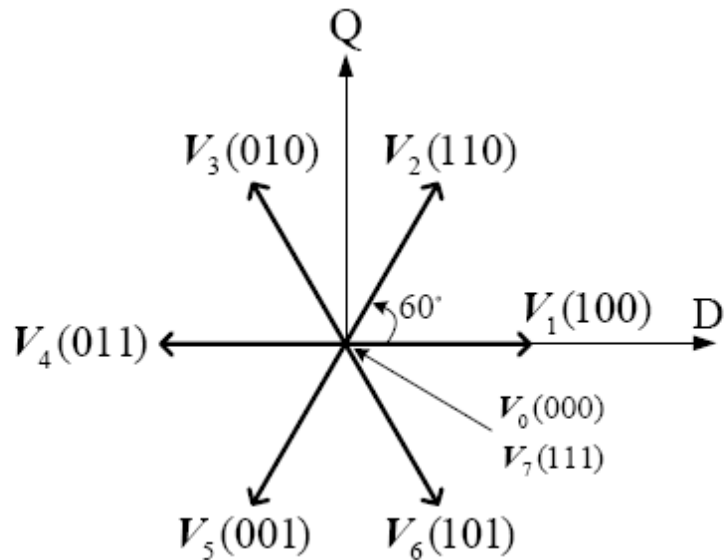


**Figure 3.1. Eight possible voltage space vectors obtained from VSI.**

The control algorithm determines a control signal whose amplitude depends on the difference between desired and actual value. This control signal can assume any value in a given interval. The three signals used in the control action of a DTC system are torque error, flux linkage error and the angle of the resultant flux linkage vector.

One revolution is divided into six sectors. In each sector the DTC chose between 4 voltage vectors. Two of the vectors increase and the other two decrease torque. Another pair of vectors increase and decrease flux. For each combination of the torque and flux hysteresis comparator states there is only one of the four voltage vectors which at the same time compensate torque and flux as desired[4].

### 3.2 TORQUE CONTROL STRATEGY IN DTC OF PMSM DRIVE:

The torque equation used for DTC of PMSM drives can be derived from the phasor diagram of conventional or permanent magnet synchronous motor shown in Fig. 3.2

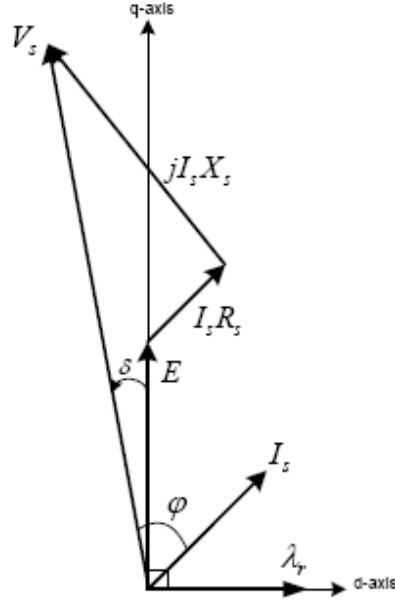


Figure 3.2. Phasor diagram of a non-salient pole synchronous machine in the motoring mode[4].

When the machine is loaded through the shaft, the motor will take real power. The rotor will then fall behind the stator rotating field. The motor current expression can be written as

$$I_s = \frac{V_s \angle 0 - E \angle \delta}{R_s + jX_s} = \frac{V_s \angle 0 - E \angle \delta}{Z_s \angle \varphi} \quad (3.1)$$

where  $|Z_s| = \sqrt{(R_s^2 + X_s^2)}$ , also  $X_s = \omega_e L_s$

$$\varphi = \tan^{-1} \left( \frac{X_s}{R_s} \right)$$

Assuming a reasonable speed such that the  $X_s$  term is higher than the resistance,  $R_s$ , such that  $R_s$  can be neglected, then  $I_s$  can then be rewritten as:

$$I_s = \frac{V_s \angle 0}{X_s} - \frac{E \angle \delta - \frac{\pi}{2}}{X_s} \quad (3.2)$$

Such that the real part of  $I_s$  is:

$$\begin{aligned} \text{Re}[I_s] &= I_s \cos \varphi = \frac{V_s}{X_s} \cos \left( -\frac{\pi}{2} \right) - \frac{E}{X_s} \cos \left( \delta - \frac{\pi}{2} \right) \\ &= -\frac{E}{X_s} \cos \left( \delta - \frac{\pi}{2} \right) = -\frac{E}{X_s} \sin \delta \end{aligned} \quad (3.3)$$

The developed power is given by:

$$P_i = 3V_s \text{Re}[I_s] = 3V_s I_s \cos \varphi \quad (3.4)$$

Substituting (3.3) into (3.4) yields:

$$P_i = -3 \frac{V_s E}{X} \sin \delta \quad \text{Watts/ph} \quad (3.5)$$

This power is positive when  $\delta$  negative, meaning that when the rotor field lags the stator field the machine is operating in the motoring region. When  $\delta > 0$  the machine is operating in the generation region. The negative sign in (3.5) can be dropped, assuming that for motoring operation a negative  $\delta$  is implied [4].

If the losses of the machine are ignored, the power  $P_i$  can be expressed as the shaft (output) power as well:

$$P_i = P_0 = \frac{2}{P} \omega_e T_{em} \quad (3.6)$$

When combining (3.5) and (3.6), the magnitude of the developed torque for a non-salient synchronous motor (or surface-mounted permanent magnet synchronous motor) can be expressed as:

$$\begin{aligned} T_{em} &= 3 \left( \frac{P}{2} \right) \frac{|V_s| |E|}{\omega_s |E|} \sin \delta \\ &= 3 \left( \frac{P}{2} \right) \frac{|\lambda_s| |\lambda_r|}{L_s} \sin \delta \end{aligned} \quad (3.7)$$

Where  $\delta$  is the torque angle between flux vectors  $\lambda_s$  and  $\lambda_r$ . If the rotor flux remains constant and the stator flux is changed incrementally by the stator voltage,  $V_s$  then the torque variation  $\Delta T_{em}$ , expression can be written as:

$$\Delta T_{em} = 3 \left( \frac{P}{2} \right) \frac{|\lambda_s + \Delta \lambda_s| |\lambda_r|}{L_s} \sin \Delta \delta \quad (3.8)$$

As it can be seen from (3.8), if the load angle,  $\delta$ , is increased then torque variation is increased [4]. To increase the load angle,  $\delta$ , the stator flux vector should turn faster than rotor flux vector. The rotor flux rotation depends on the mechanical speed of the rotor, so to decrease load angle,  $\delta$ , the stator flux should turn slower than rotor flux. Therefore, according to the torque (3.7), the electromagnetic torque can be controlled effectively by controlling the amplitude and rotational speed of stator flux vector,  $\lambda_s$ . To achieve the above phenomenon, appropriate voltage vectors are applied to the motor terminals. For counter-clockwise operation, if the actual torque is smaller than the reference value, then the voltage vectors that keep the stator flux vector,  $\lambda_s$ , rotating in the same direction are selected. When the load angle,  $\delta$ , between  $\lambda_s$  and  $\lambda_r$  increases the actual torque increases as well. Once the actual torque is greater than the reference value, the voltage vectors that keep stator flux vector,  $\lambda_s$ , rotating in the reverse direction are selected instead of the zero voltage vectors. At the same time, the load angle,  $\delta$ , decreases thus the torque decreases.

### 3.3 FLUX CONTROL STRATEGY OF PMSM DRIVE:

If the resistance term in the stator flux estimation algorithm is neglected, the variation of the stator flux linkage (incremental flux expression vector) will only depend on the applied voltage vector as shown in Fig. 3.3

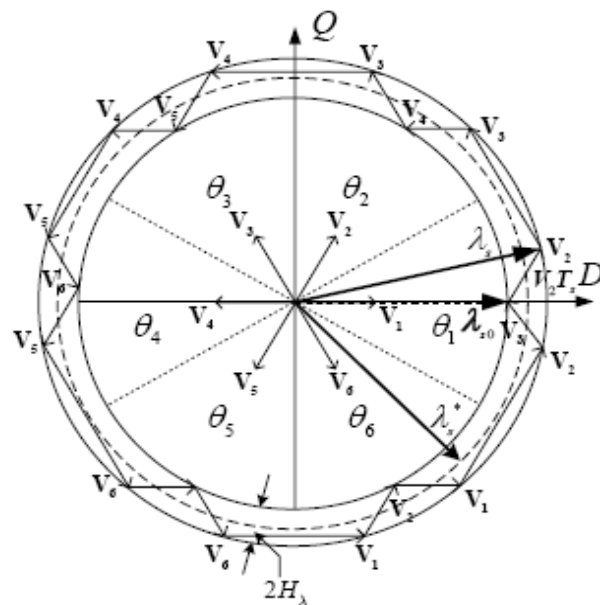


Figure 3.3. Incremental stator flux linkage space vector representation in the DQ-plane.

For a short interval of time, namely the sampling time,  $T_s = \Delta t$ , the stator flux linkage,  $\lambda_s$  position and amplitude can be changed incrementally by applying the stator voltage vector,  $V_s$ . As discussed above, the position change of the stator flux linkage vector,  $\lambda_s$ , will affect the torque. The stator flux linkage of a PMSM that is depicted in the stationary reference frame is written as:

$$\lambda_s = \int (V_s - R_s i_s) dt \quad (3.9)$$

During the sampling interval time or switching interval, one out of the six voltage vectors is applied, and each voltage vector applied during the pre-defined sampling interval is constant, eqn (3.9) can be rewritten as

$$\lambda_s = V_s t - R_s \int i_s dt + \lambda_{s|t=0} \quad (3.10)$$

Where  $\lambda_{s|t=0}$ , is the initial stator flux linkage at the instant of switching,  $V_s$ , is the measured stator voltage,  $i_s$ , is the measured stator current, and  $R_s$ , is the estimated stator resistance. When the stator term in stator flux estimation is removed implying that the end of the stator flux vector,  $\lambda_s$ , will move in the direction of the applied voltage vector, as shown in Fig. 3.3, we obtain:

$$\Delta \lambda_s = V_s \Delta t \quad (3.11)$$

The goal of controlling the flux in DTC is to keep its amplitude within a pre-defined hysteresis band. By applying a required voltage vector stator flux linkage amplitude can be controlled [7]. To select the voltage vectors for controlling the amplitude of the stator flux linkage the voltage plane is divided into six regions, as shown in Fig. 3.3.

In each region two adjacent voltage vectors, which give the minimum switching frequency, are selected to increase or decrease the amplitude of stator flux linkage, respectively. For example, according to the Table I, when the voltage vector  $V_2$ , is applied in Sector 1, then the amplitude of the stator flux increases when the flux vector rotates counter-clockwise. If  $V_3$ , is selected then stator flux linkage amplitude decreases.

Fig. 3.4 is a basic graph that shows how flux and torque can be changed as a function of the applied voltage vector. According to the figure, the direct component of applied voltage vector changes the amplitude of the stator flux linkage and the indirect

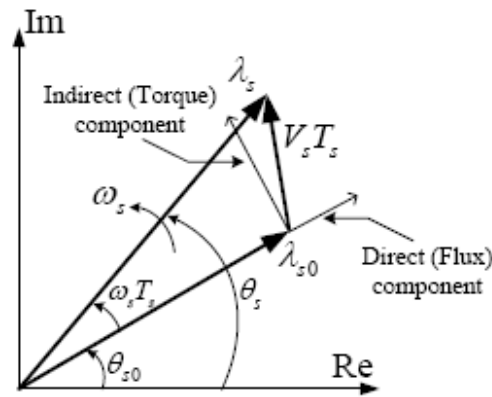


**Figure 3.4. Representation of direct and indirect components of the stator flux linkage vector[4].**

component changes the flux rotation speed which changes the torque [8]. If the torque needs to be changed abruptly then the flux does as well, so the closest voltage vector to the indirect component vector is applied. If torque change is not required, but flux amplitude is increased or decreased then the voltage vector closest to the direct component vector is chosen. Consequently, if both torque and flux are required to change then the appropriate resultant mid-way voltage vector between the indirect and direct components is applied. It seems obvious from (3.9) that the stator flux linkage vector will stay at its original position when zero voltage vectors  $S_a$  (000) and  $S_b$  (111) are applied. This is true for an induction motor since the stator flux linkage is uniquely determined by the stator voltage. On the other hand, in the DTC of a PMSM, the situation of applying the zero voltage vectors is not the same as in induction motors. This is because the stator flux linkage vector will change even when the zero voltage vectors are selected since the magnets rotate with the rotor [9]. As a result, the zero voltage vectors are not used for controlling the stator flux linkage vector in a PMSM. In other words, the stator flux linkage should always be in motion with respect to the rotor flux linkage vector.

### **3.4 VOLTAGE VECTOR SELECTION IN DTC OF PMSM DRIVE:**

As discussed before, the stator flux is controlled by properly selected voltage vectors, and as a result the torque by stator flux rotation. The higher the stator vector rotation speed the faster torque response is achieved.

The estimation of the stator flux linkage components described previously requires the stator terminal voltages. In a DTC scheme it is possible to reconstruct those voltages from the DC-link voltage,  $V_{dc}$ , and the switching states ( $S_a, S_b, S_c$ ) of a six-step voltage-source inverter (VSI) rather than monitoring them from the motor terminals [8]-[9]. The primary voltage vector,  $V_s$ , is defined by the following equation:

$$v_s = (2/3)(v_a + v_b e^{j(2/3)\pi} + v_c e^{j(4/3)\pi}) \quad (3.12)$$

where,  $v_a, v_b$  and  $v_c$  are the instantaneous values of the primary line-to-neutral voltages. When the primary windings are fed by an inverter, as shown in Fig. 3.5, the primary voltages  $v_a, v_b$  and  $v_c$  are determined by the status of the three switches,  $S_a, S_b$  and  $S_c$ . If the switch is at state 0 that means the phase is connected to the negative and if it is at 1 it means that the phase is connected to the positive leg.

For example,  $v_a$  is connected to  $V_{dc}$  if  $S_a$  is one, otherwise  $v_a$  is connected to zero. This is similar for  $v_b$  and  $v_c$ . The voltage vectors that are obtained this way are shown in Fig. 3.1. There are six nonzero voltage vectors:  $V_1(100)$ ,  $V_2(110)$ , ..., and  $V_6(101)$  and two zero voltage vectors:  $V_7(000)$  and  $V_8(111)$ . The six nonzero voltage vectors are  $60^\circ$  apart from each other as in Fig. 3.1.

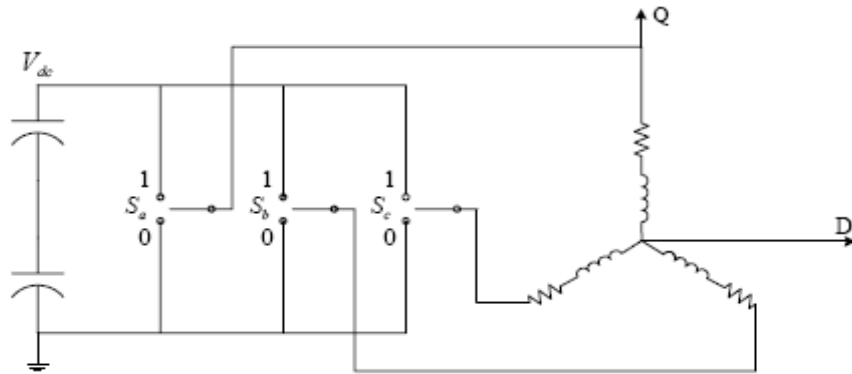


**Figure 3.5. Voltage source inverter (VSI) connected to the R-L load.**

The stator voltage space vector (expressed in the stationary reference frame) representing the eight voltage vectors can be shown by using the switching states and the DC-link voltage,  $V_{dc}$ , as:

$$v_s(S_a, S_b, S_c) = (2/3)V_{dc}(S_a + S_b e^{j(2/3)\pi} + S_c e^{j(4/3)\pi}) \quad (3.13)$$

Where  $V_{dc}$ , is the DC-link voltage and the coefficient of 2/3 is the coefficient comes from the Park's Transformation. Equation (3.13) can be derived by using the line-to-line voltages of the AC motor which can be expressed as:

$$v_{ab} = V_{dc}(S_a - S_b), v_{bc} = V_{dc}(S_b - S_c), v_{ca} = V_{dc}(S_c - S_a) \quad (3.14)$$

The stator phase voltages (line-to-neutral voltages) are required for (3.12). They can be obtained from the line-to-line voltages as.

$$v_a = (v_{ab} - v_{ca})/3, v_b = (v_{bc} - v_{ab})/3, v_c = (v_{ca} - v_{bc})/3 \quad (3.15)$$

If the line-to-line voltages in terms of the DC-link voltage,  $V_{dc}$ , and switching states are substituted into the stator phase voltages it gives:

$$\begin{aligned} v_a &= (1/3) V_{dc}(2S_a - S_b - S_c) \\ v_b &= (1/3) V_{dc}(-S_a + 2S_b - S_c) \\ v_c &= (1/3) V_{dc}(-S_a - S_b + 2S_c) \end{aligned} \quad (3.14)$$

Equation (3.14) can be summarized by combining with (3.12) as:

$$\begin{aligned} v_a &= \text{Re}(v_s) = (1/3) V_{dc}(2S_a - S_b - S_c) \\ v_b &= \text{Re}(v_s) = (1/3) V_{dc}(-S_a + 2S_b - S_c) \\ v_c &= \text{Re}(v_s) = (1/3) V_{dc}(-S_a - S_b + 2S_c) \end{aligned} \quad (3.15)$$

To determine the proper applied voltage vectors, information from the torque and flux hysteresis outputs, as well as stator flux vector position, are used so that circular stator flux vector trajectory is divided into six symmetrical sections according to the non zero voltage vectors as shown in Fig. 3.3 [4].

According to Fig. 3.6, while the stator flux vector is situated in sector  $i$ , voltage vectors  $V_{i+1}$  and  $V_{i-1}$  have positive direct components, increasing the stator flux amplitude, and  $V_{i+2}$  and  $V_{i-2}$  have negative direct components, decreasing the stator flux amplitude. Moreover,  $V_{i+1}$  and  $V_{i+2}$  have positive indirect components, increasing the torque

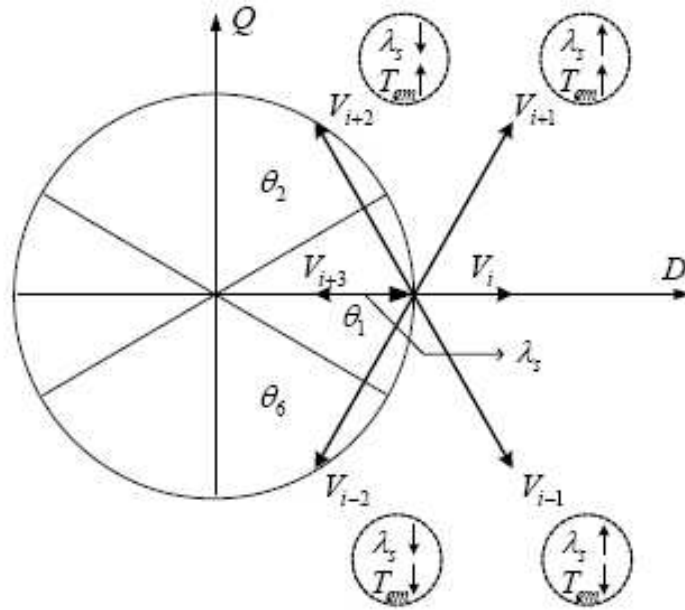


**Figure 3.6. Voltage vector selection when the stator flux vector is located in sector  $i$ .**

response, and  $V_{i-1}$  and  $V_{i-2}$  have negative indirect components, decreasing the torque response. In other words, applying  $V_{i+1}$  increases both torque and flux but applying  $V_{i+1}$  increases torque and decreases flux amplitude.

The switching table for controlling both the amplitude and rotating direction of the stator flux linkage is given in Table I [13]. The voltage vector plane is divided into six sectors so that each voltage vector divides each region into two equal parts. In each sector, four of the six non-zero voltage vectors may be used [13]. Zero vectors are also allowed. All the possibilities can be tabulated into a switching table. The switching table is shown in Table I. The output of the torque hysteresis comparator is denoted as  $\tau$ , the output of the flux hysteresis comparator as  $\psi$  and the flux linkage sector is denoted as  $\theta$ . The torque hysteresis comparator is a two valued comparator;  $\tau = 0$  means that the actual value of the torque is above the reference and out of the hysteresis limit and  $\tau = 1$  means that the actual value is below the

reference and out of the hysteresis limit. The flux hysteresis comparator is a two valued comparator as well where  $\psi = 1$  means that the actual value of the flux linkage

**Table 3.1. Switching table**

$\Psi$	T	$\theta$					
		$\theta(1)$	$\theta(2)$	$\theta(3)$	$\theta(4)$	$\theta(5)$	$\theta(6)$
$\Psi=1$	T=1	$V_2(110)$	$V_3(010)$	$V_4(011)$	$V_5(001)$	$V_6(101)$	$V_3(010)$
	T=0	$V_6(101)$	$V_1(100)$	$V_2(110)$	$V_3(010)$	$V_4(011)$	$V_5(001)$
$\Psi=0$	T=1	$V_3(010)$	$V_4(011)$	$V_5(001)$	$V_6(101)$	$V_1(100)$	$V_2(110)$
	T=0	$V_5(001)$	$V_6(101)$	$V_1(100)$	$V_2(110)$	$V_3(010)$	$V_4(011)$

is below the reference and out of the hysteresis limit and  $\psi = 0$  means that the actual value of the flux linkage is above the reference and out of the hysteresis limit. Rahman et al have suggested that no zero vectors should be used with a PMSM. Instead, a non zero vector which decreases the absolute value of the torque is used. Their argument was that the application of a zero vector would make the change in torque subject to the rotor mechanical time constant which may be rather long compared to the electrical time constants of the system. This results in a slow change of the torque [7], [9].

We define  $\psi$  and  $\tau$  to be the outputs of the hysteresis controllers for flux and torque, respectively, and  $\theta(1) - \theta(6)$  as the sector numbers to be used in defining the stator flux linkage positions. In Table I, if  $\psi = 1$ , then the actual flux linkage is smaller than the reference value. On the other hand, if  $\psi = 0$ , then the actual flux linkage is greater than the reference value. The same is true for the torque.

### 3.5 CONVENTIONAL DIRECT TORQUE CONTROL SYSTEM:

In this section the basic DTC control system is presented in detail and the functions of all system blocks are explained. Figure 3.7 shows the block diagram of the DTC. Each block is described in detail below.

Let's start with the motor currents and follow the signals around the system to the Voltage Source Inverter output.

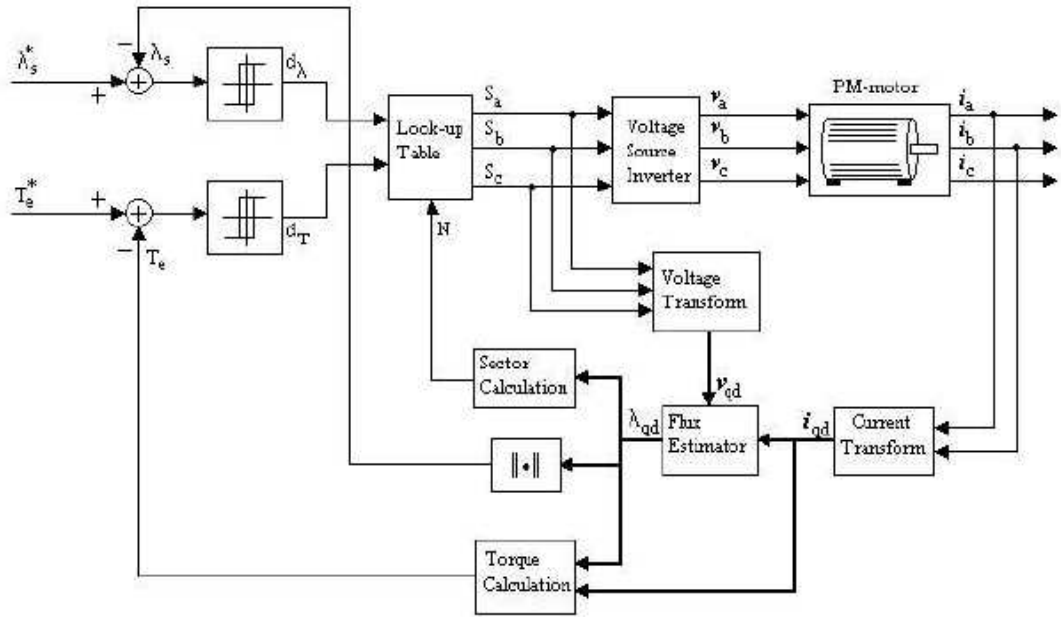


Figure 3.7. Classical DTC scheme.

### 3.5.1 CURRENT TRANSFORM:

As seen in the figure only two of the input currents are sensed. The motor in a drive system is normally operated with its neutral point floating, in this case  $i_a + i_b + i_c = 0$  so the current not sensed is given of them other two. The  $i_{abc}$  current is then transformed to its quadrature and direct axes components according to the Park Transformation.

In chapter two the abc-components were transformed into the rotor reference frame and absolute rotor position was supposed to be known. In reality there is a desire of not using rotor position explicitly because this implies the use of angular encoders. In the DTC system, variables are transformed into the  $\alpha\beta$  stator reference frame, which does not make use of any angular information.

This transformation becomes a simple mapping

$$\begin{bmatrix} i_{\alpha} \\ i_{\beta} \\ i_0 \end{bmatrix} = \begin{bmatrix} \frac{2}{3} & -\frac{1}{3} & -\frac{1}{3} \\ 0 & -\frac{1}{\sqrt{3}} & \frac{1}{\sqrt{3}} \\ 0 & 0 & 0 \end{bmatrix} \begin{bmatrix} i_a \\ i_b \\ i_c \end{bmatrix} \quad (3.16)$$

The zero component is left since, when the neutral floats there is no need to consider it.

### 3.5.2 FLUX ESTIMATOR:

Now that the current,  $i_{\alpha\beta}$ , is known, the signal continues in to the flux estimator. In to this block also enters the VSI voltage vector transformed to the  $\alpha\beta$ -stationary reference frame. The voltage,  $V_{\alpha\beta}$ , is calculated as in eqn.3.16 so no further explanation is needed.

The dq-voltage eqn's with zero components left is

$$V_{dq} = R_s i_{dq} + \omega_r \begin{bmatrix} -\lambda_q \\ \lambda_d \end{bmatrix} + \frac{d}{dt} \lambda_{dq} \quad (3.17)$$

One can directly obtain a means for stator flux estimation by noting that  $w_r=0$  and rearranging

$$\lambda_{\alpha\beta} = \int (V_{\alpha\beta} - R_s i_{\alpha\beta}) dt \quad (3.18)$$

This formula is the foundation of implementing the flux estimator.

### 3.5.3 TORQUE ESTIMATOR:

The torque in the PMSM motor drive rotor reference frame is given by

$$T_e = (3/4)P(\lambda_d i_q - \lambda_q i_d) \quad (3.19)$$

which is true for all dq-reference frames. The torque in PMSM motor is estimated from the calculated currents and fluxes in the stationary  $\alpha\beta$ -reference frame. To calculate torque one only has to substitute the corresponding, already, calculated fluxes and currents. Torque calculation is thus a simple operation.

### 3.5.4 SECTOR CALCULATION:

The control action taken by the DTC control is based on the states of the flux and torque hysteresis comparators. Flux is increased by applying a vector pointing in the  $\lambda_{dq}$

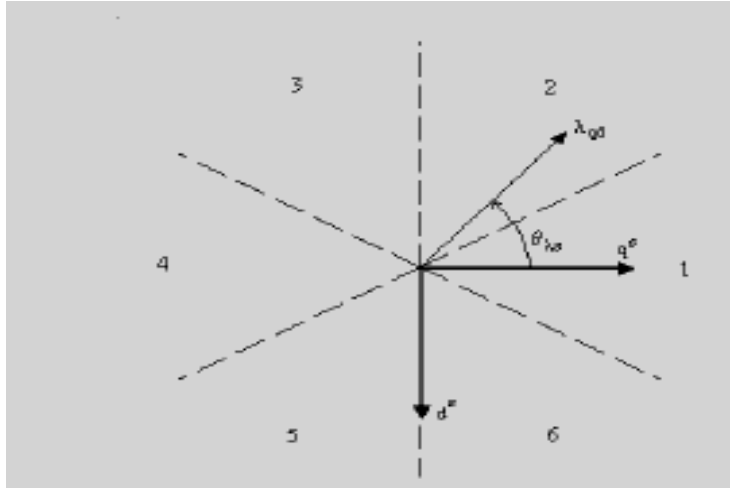


**Figure 3.8. DTC sectors and reference frames.**

direction and torque is increased by applying a vector pointing in the rotational direction. In order to do so, the angular position of the stator flux vector must be known so that the DTC can choose between an appropriate set of vectors depending on the flux position.

Each sector spans  $60^\circ$  degrees, the sectors are numbered as in fig 3.8.

As seen from the fig the angle  $\theta$  can be found from:

$$\theta = \tan^{-1}(\lambda_\beta / \lambda_\alpha) \quad (3.20)$$

If  $\lambda_{dq}$  belongs to sector 1, switch vectors  $v_2$ ,  $v_3$ ,  $v_5$  and  $v_6$  are used.

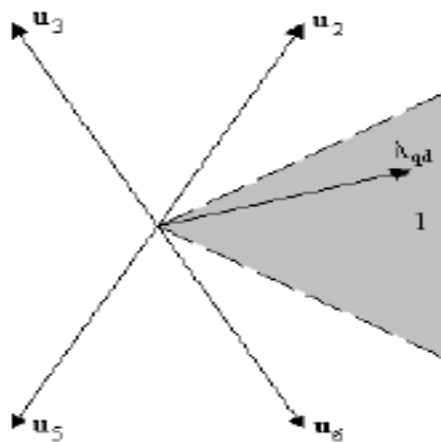


**Figure 3.9. VSI vectors used when  $\lambda_{dq}$  is in sector 1.**

### 3.5.5 TORQUE AND FLUX HYSTERESIS COMPARATORS:

Now we know in which sector is the flux and its norm, and we also know how much torque the motor develops. Estimated torque and flux are compared to their command values. The difference between command and estimated value is compared in the hysteresis comparators.

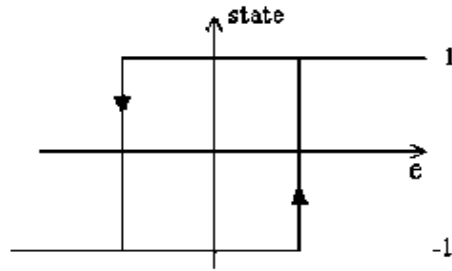


Figure 3.10. 2-level hysteresis comparator[10].

### 3.5.6 LOOK –UP TABLE:

The hysteresis comparator states,  $d_T$  and  $d_\phi$ , together with the sector number,  $N$ , are now used by the Look-up Table block to chose an appropriate voltage vector.

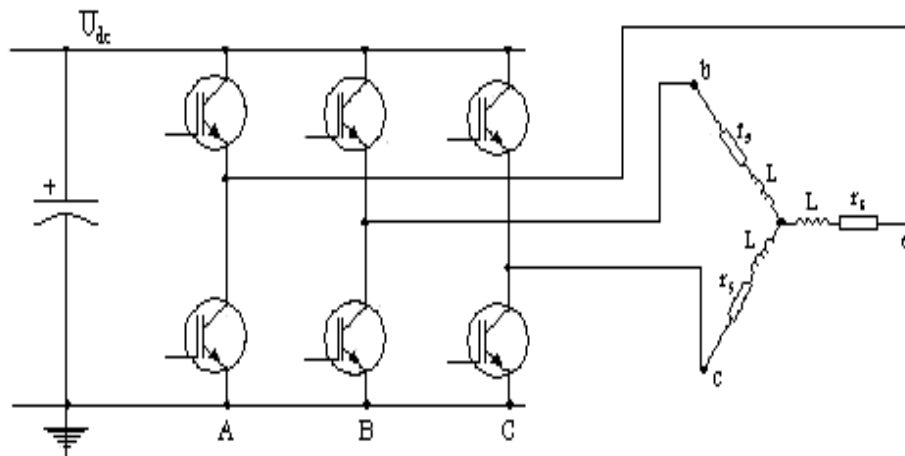
A table frequently used in DTC when controlling a Permanent Magnet motor is shown in table 3.2,

Table 3.2. Voltage Vector Switching Table

		N					
$D\lambda$	$d\tau$	1	2	3	4	5	6
-1	-1	$U_5$	$U_6$	$U_1$	$U_2$	$U_3$	$U_4$
	1	$U_3$	$U_4$	$U_5$	$U_6$	$U_1$	$U_2$
1	-1	$U_6$	$U_1$	$U_2$	$U_3$	$U_4$	$U_5$
	1	$U_2$	$U_3$	$U_4$	$U_5$	$U_6$	$U_1$

The selected voltage vector is applied at the gate of the Voltage source inverter (VSI).

### 3.5.7 VOLTAGE SOURCE INVERTER:



**Figure 3.11. VSI and how the motor windings are connected.**

The VSI synthesizes the voltage vectors commanded by the look up table block. In the case of DTC this task is quite simple since no pulse width modulation is used; the output devices stay in the same state during the entire sampling period.

Figure 3.11 shows a simplified sketch of the VSI output stage, and how the motor windings are connected.

The output-signals from the Look-up Table block in Fig. 3.7 are named  $S_a$ ,  $S_b$  and  $S_c$ . These are Boolean variables indicating the switch state in the inverter output-branches.

Let  $S_i = 1$  when the high or upper switch is on and the lower is off, and  $S_i = 0$  when the lower is on and upper is off. The inverter states ( $S_a S_b S_c$ ), generating each voltage vector then are:

$$u_1 = (1\ 0\ 0), u_2 = (1\ 1\ 0), u_3 = (0\ 1\ 0), u_4 = (0\ 1\ 1), u_5 = (0\ 0\ 1), u_6 = (1\ 0\ 1)$$

The VSI inverter terminals are connected to motor abc terminals.

### **3.6 ADVANTAGES AND DISADVANTAGES OF THE DIRECT TORQUE CONTROL TECHNIQUE:**

There are many advantages of direct torque control over other high-performance torque control systems such as vector control. Some of these are summarized as follows [10]:

- The only parameter that is required is stator resistance
- The switching commands of the inverter are derived from a look-up table, simplifying the control system and also decreasing the processing time unlike a PWM modulator used in vector control.
- Instead of current control loops, stator flux linkage vector and torque estimation are required so that simple hysteresis controllers are used for torque and stator flux linkage control.
- Vector transformation is not applied because stator quantities are enough to calculate the torque and stator flux linkage as feedback quantities to be compared with the reference values.

Although there are several advantages of the DTC scheme over vector control, it still has a few drawbacks which are explained below:

- A major drawback of the DTC scheme is the high torque and stator flux linkage ripples. Since the switching state of the inverter is updated once every sampling time, the inverter keeps the same state until the outputs of each hysteresis controller changes states. As a result, large ripples in torque and stator flux linkage occur.
- The switching frequency varies with load torque, rotor speed and the bandwidth of the two hysteresis controllers.
- Stator flux estimation is achieved by integrating the difference between the input voltage and the voltage drop across the stator resistance. The applied voltage on the motor terminal can be obtained either by using a DC-link voltage sensor, or two voltage sensors connected to the any two phases of the motor terminals. For current sensing there

should be two current sensors connected on any two phases of the motor terminals. Offset in the measurements of DC-link voltage and the stator currents might happen, because for current and voltage sensing, however, temperature sensitive devices, such as operational amplifiers, are normally used which can introduce an unwanted DC offset. This offset may introduce large drifts in the stator flux linkage computation (estimation) thus creating an error in torque estimation (torque is proportional to the flux value) which can make the system become unstable.

- The stator flux linkage estimation has a stator resistance, so any variation in the stator resistance introduces error in the stator flux linkage computation, especially at low frequencies. If the magnitude of the applied voltage and back-EMF are low, then any change in the resistance will greatly affect the integration of the back-EMF.
- Because of the constant energy provided from the permanent magnet on the rotor the rotor position of motor will not necessarily be zero at start up. To successfully start the motor under the DTC scheme from any position (without locking the motor at a known position), the initial position of the rotor magnetic flux must be known. Once it is started properly, however, the complete DTC scheme does not explicitly require a position sensor.

### **3.7 SUMMARY:**

In this chapter a theoretical review of DTC for applying to a PMSM motor is given. An algorithm for implementation of Direct Torque control technique for a two level inverter driving PMSM motor is developed. The key elements like torque estimation, flux estimation and voltage vector selection table is also given.

# **Chapter 4**

## **Three Level Voltage Source Inverter**

## Chapter 4

### THREE LEVEL VOLTAGE SOURCE INVERTER

#### 4.1 INTRODUCTION

Multi level inverters, such as three level inverters, are an emerging technology and are commonly applied to high power motion drives instead of the standard two-level voltage source inverters (VSI). In three-level inverters the blocking voltage of each switch is half of the DC bus voltage, lower  $dV/dt$  is generated and the output voltage and current have lower harmonic distortion.. In the three level inverter the voltage selection possibilities are enhanced since more inverter states are available. In this chapter the application of the Direct Torque Control (DTC) strategy is studied for this particular topology and the switching table adapted for applying three level inverter to the conventional DTC is discussed.

#### 4.2 THE THREE LEVEL NEUTRAL POINT CLAMPED INVERTER

A multilevel voltage source inverter is a converter structure that can provide more than two levels of line to ground voltage in the output of each leg of the inverter. Multilevel power conversion technology is a very fast growing area of power electronics with good potential for further development. The most attractive features of this technology are in the medium to high-voltage application range of (2-13KV), which includes motor drives, power distribution, power quality and power conditioning applications. Different circuit topologies have been implemented in multilevel inverters. One of the most used of these topologies is the Neutral point Clamped (NPC) topology. In Fig 4.1 the scheme for the three level inverter is presented. In Fig 4.2, the different vectors or inverter states available, in a three level inverter, are shown in the stator flux locus [18]. As can be seen, there are 4 different kinds of vectors

- Zero vectors:  $V_z$  (with 3 possible configurations).

- Large vectors:  $V_{1L}, V_{2L}, V_{3L}, V_{4L}, V_{5L}, V_{6L}$ .
- Medium vectors:  $V_{1m}, V_{2m}, V_{3m}, V_{4m}, V_{5m}, V_{6m}$ .
- Small vectors:  $V_{1s}, V_{2s}, V_{3s}, V_{4s}, V_{5s}, V_{6s}$  (with 2 possible configurations for each).

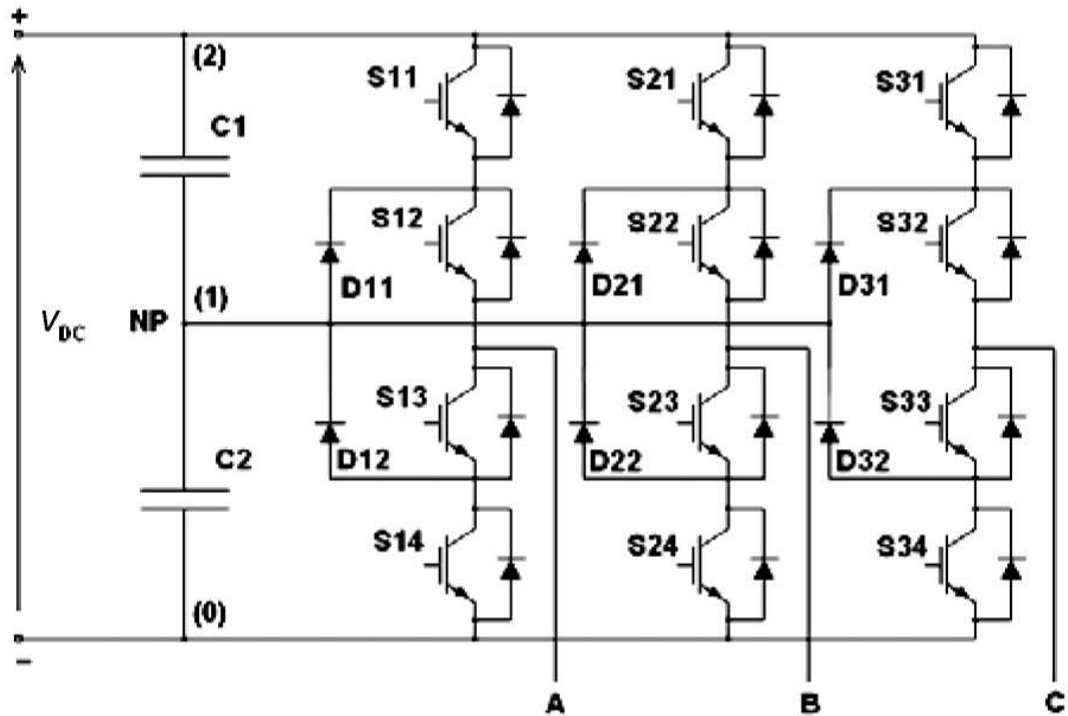


Figure 4.1. Three level NPC inverter[21].

Although in a three level inverter there are 27 possible states, some of them apply the same voltage vector [21]. There are two possible configurations for each small vector and three for the zero vector  $V_z$ . Therefore, 19 different vectors are available in a three level inverter  $V_z$  to  $V_{6s}$ . The state of the switches for each leg is shown in brackets (2: phase connected to the positive of the DC-link; 1: phase connected to the middle point of the DC-link (Neutral point NP); 0: phase connected to the negative of the DC link).

### 4.3 DTC WITH A THREE LEVEL INVERTER

In direct torque control, the torque and the stator flux are regulated to their reference value by selecting the adequate switching state. The conventional DTC with a two level inverter makes no difference between large and small flux and torque errors. The switching states chosen for the large error that occurs during the start up or during a step change in torque or flux reference are the same that have been chosen for the fine control during steady state. A better quantification of the input variables increasing the number of levels of the Hysteresis blocks together with splitting the stator flux position in to 6 sectors and the increased number of inverter states available for a three level inverter may lead to a better performance of the control [14].

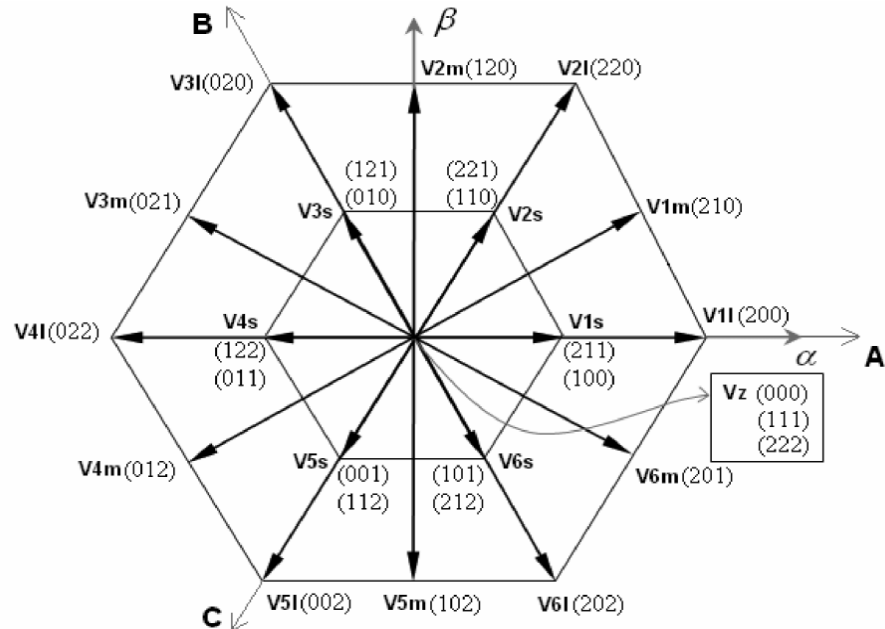


Figure 4.2. Voltage space vectors for a three level NPC inverter[21].

### 4.4 VECTOR SELECTION TABLE FOR THREE LEVEL INVERTER

The proposed DTC algorithm, which is employed with a 3-level inverter, is a natural extension of the classical DTC to multilevel inverters. With an inverter shown in fig 4.1 the possible inverter switching states, for each phase, are shown in Tab.4.1 where  $S_x$  is a variable which identifies the switching state of an inverter leg. Each voltage space vector generated by the inverter is then identified by a 3-component vector, like (2 2 1), where

each component is given by the value of  $S_x$ , for each of the three legs of the inverter: Fig 4.2 shows the hexagon of the 19 voltage space vectors which can be generated by such an inverter. The proposed DTC algorithm employs only 12 active voltage space vectors, divided into two categories on the basis of the parameter  $Lev_u$  (voltage level) as shown in Tab.4.2, without using either the null space vector, for dynamical reasons as explained later in this paragraph, or the active vectors (210 102 120 201 021 012), which are characterized by three different numbers, for capacitor balancing reasons [14].

**Table 4.1. Switching states of a three level inverter**

SxA	S1A	S2A	S3A	S4A
2	On	On	Off	Off
1	Off	On	On	Off
0	Off	Off	On	On

As it can be seen from Tab.4.2, any  $U_i$  space vector (with  $i=1, 2, \dots, 6$ ) with  $Lev_u = \text{low}$  can be obtained with two different switching patterns and this is exploited to avoid the capacitor voltage unbalance, as shown in Table 4.3.

**Table 4.2. Voltage space vectors employed in the proposed DTC algorithm**

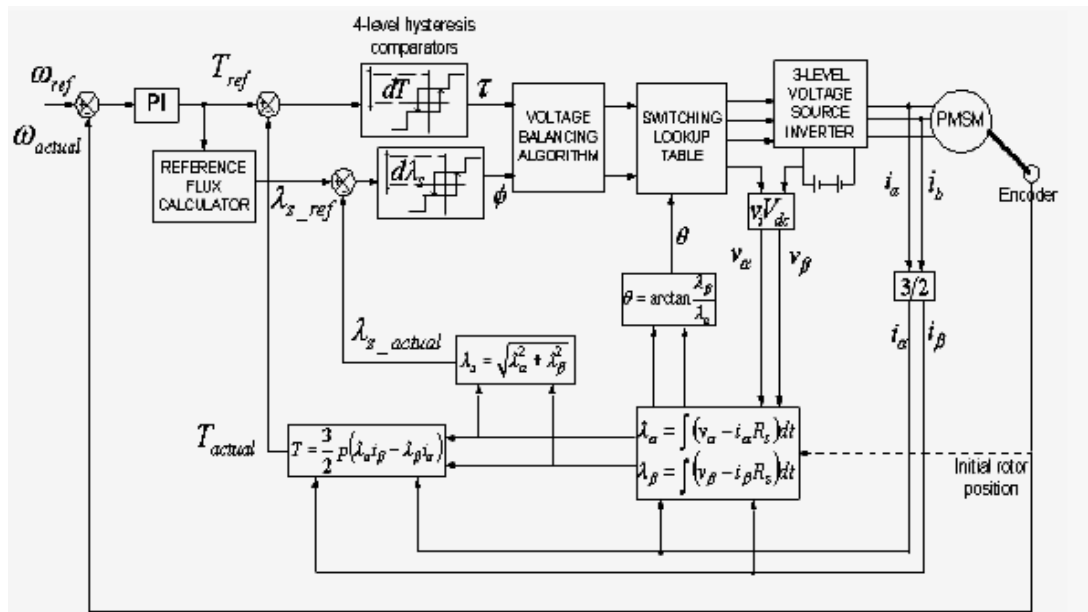
		U1	U2	U3	U4	U5	U6
$Lev_u$	High	2 0 0	2 2 0	0 2 0	0 2 2	0 0 2	2 0 2
	Low	2 1 1	2 2 1	1 2 1	1 2 2	1 1 2	2 1 2
	Low	1 0 0	1 1 0	0 1 0	0 1 1	0 0 1	1 0 1

**Table 4.3. Adopted control strategy**

	Te↑ $\psi_s$ ↑	Te↑ $\psi_s$ ↓	Te↓ $\psi_s$ ↑	Te↓ $\psi_s$ ↓
Control strategy ( $\theta$ sector)	$U_{i+1}$	$U_{i+2}$	$U_{i-1}$	$U_{i-2}$

(arrow up= increase, arrow down= decrease)

The employed DTC block diagram, shown in Fig. 4.3, is the natural extension of classical DTC. It shows that the closed loop control of both the rotor speed and the stator flux linkage is performed. Speed control is done by employing a PI controller which processes the speed error obtained as difference between the reference speed and the measured one (obtained by the encoder in Fig. 4.3) its output is the reference torque. Both torque and stator flux controls are achieved by using 4-level hysteresis comparators the output of this comparator ( $T_{out}$  for the torque and  $\psi_{out}$  for the stator-flux linkage) can be either 2 (-2) or 1 (-1) according to the positive (negative) value of the torque or the flux error: if the value of the error is within the hysteresis loop, then the output of the comparator is 1 (-1) if the previous comparator output was 1 or 2 (-1 or -2). On the basis of the sector  $\theta$  ( $\theta=1, 2, \dots, 6$ ) in which the stator flux linkage lies and of the magnitude of



errors of the torque and flux loops, a voltage space vector  $U_i$  (with  $i=1, 2, \dots, 6$ ) is generated. In this control strategy no null vector has been used to obtain the best dynamical performances of the electrical drive, at the expenses though of higher ripples in the torque. If the absolute value of the output of one of the two the comparators is

Figure 4.3. Schematic diagram of the DTC PMSM drive system for Three-level inverter[15].

higher than two, then the voltage space vector  $U$ , with  $Lev_u="high"$  is generated, otherwise  $U$ , with  $Lev_u="low"$  is selected. As clearly shown in Fig. 4.4, the effect of the

voltage space vector with  $Lev_u = \text{''high''}$  is to cause high variations both in the torque and in the stator flux, while the effect of the voltage space vector with  $Lev_u = \text{''low''}$  is to cause smaller variations. The use of more voltage vectors in the 3-level inverter fed DTC than in the 2-level inverter fed DTC permits therefore a corresponding reduction of the harmonic content in stator voltages and currents.

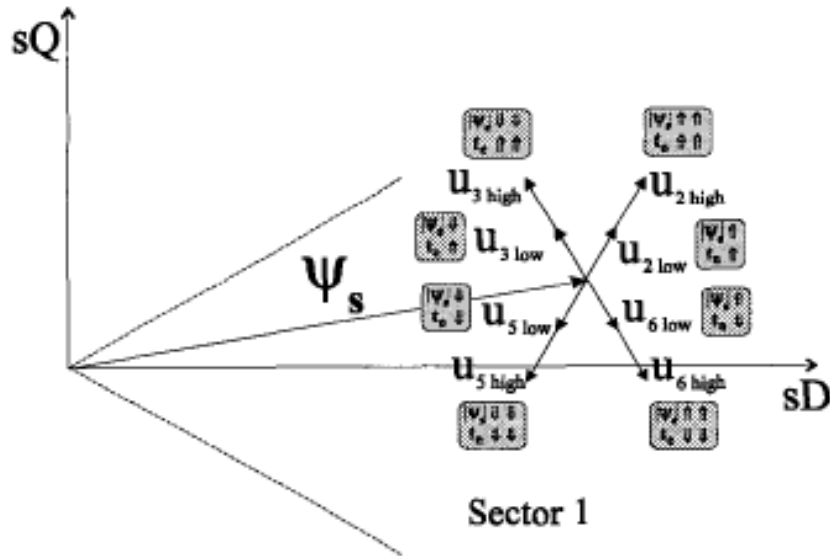


Figure 4.4. Effect of voltage space vectors on torque and stator flux linkages[14].

(arrow up= increase, double arrow up= strong increase

arrow down= decrease, double arrow down= strong decrease)

The stator flux linkage amplitude is estimated with a classical open-loop “voltage model based on the well known stator equations of the PMSM machine [14]:

$$\begin{cases} \Psi_{sD} = \int (u_{sD} - R_s i_{sD}) dt \\ \Psi_{sQ} = \int (u_{sQ} - R_s i_{sQ}) dt \end{cases}$$

In the control scheme the stator voltage components are computed on-line from the knowledge of the DC-link voltage and the switching state  $S_{xA}$ ,  $S_{xB}$ ,  $S_{xC}$  of the upper devices of the legs of the inverter with the following formulae [14]:

$$\begin{cases} u_{sA} = U_d/6(2S_{xA} - S_{xB} - S_{xC}) \\ u_{sB} = U_d/6(2S_{xB} - S_{xA} - S_{xC}) \\ u_{sC} = U_d/6(2S_{xC} - S_{xA} - S_{xB}) \end{cases}$$

The electromagnetic torque is estimated on-line by the knowledge of the instantaneous values of the direct and quadrature stator flux linkage and current components:

$$t_e = (3/2)p(\Psi_{sD} i_{sQ} - \Psi_{sQ} i_{sD})$$

It should be remarked that the final switching pattern is selected on the basis of the elaboration of the “voltage balancing algorithm”, as described in the next section.

#### 4.5 CONTROL ALGORITHM FOR DC LINK CAPACITOR VOLTAGES BALANCING

In the three-level inverter topology the DC link capacitor voltage balancing problem is inherent. It is required that two DC link capacitor voltages (C1 and C2 in Fig. 4.1) should be maintained balanced to guarantee three-level operation throughout the whole output voltage range. For this, a switching pattern should be properly selected.

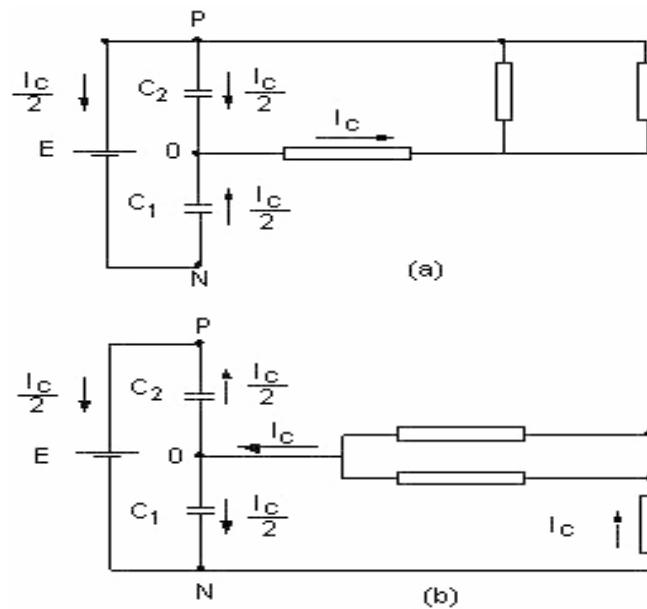


Figure 4.5. Voltage unbalancing of the inverter capacitors[15].

If it is violated, the output of the inverter will contain even order harmonics that are fatal in AC drives. Among the voltage space vectors selected in this case, the full vectors, do not unbalances the capacitors voltage because its configurations that connects the motor windings with positive or negative points, the half vectors unbalances the capacitors due to it's the configurations that connects to middle point as shown in the Fig. 4.5.

This figure shows the effect of the voltage space vector  $V_{2,\text{half}}$  on the capacitors voltage balancing where the same voltage space vector can be generated with two possible switching patterns (221) and (110) and one of them connect the motor windings between the points 2 and 1 of the DC link

while the other connects them between the points 1 and 0 of the inverter. The switching configuration in Figs. (4.5a) and (4.5b) has opposite effects on the voltage unbalance of the capacitors  $C_1, C_2$  in steady state. Due to one possible switching state the voltage space vectors of the medium category such as (201) unbalance the capacitors and ones are not used. The zero voltage space vectors are not used also to PMSM like explained in the previous section.

The voltage balancing algorithm and the consequent switching pattern selection which takes into account the voltage balance is shown now. If the values of the torque error output or flux error output are larger than positive hysteresis band ( $dT$  or  $d\lambda_s$ ) or less than negative hysteresis band ( $-dT$  or  $-d\lambda_s$ ) then a voltage space vector with level full is selected as well as the corresponding switching state, otherwise, if error values is more than zero and less than positive hysteresis band or if it is less than zero and more than negative hysteresis band, to avoid capacitor voltage unbalance a voltage space vector with level half is selected, then the sign of the current provided by the DC link is compared with the one of the last instant when a level half vector had been applied (algorithm memorizes the kind of the switching pattern in the last instant  $k$  in which a level half vector had been applied) and, if the sign of the current does not change, then the other switching pattern type for level half is selected to permit the capacitor voltages to be balanced [15].

#### **4.6 SUMMARY**

This chapter presents the direct torque control concept using three-level inverter. The voltage vector selection criterion for a three level inverter is discussed and a control algorithm for voltage unbalancing problem in a three level inverter is developed.

# **Chapter 5**

## **Simulation Results**

## Chapter 5

### SIMULATION RESULTS

#### 5.1 INTRODUCTION:

The control system block diagrams shown in Fig 3.7 and Fig 4.3 and simulated for Permanent Magnet Synchronous Motor in the Matlab-Simulink environment. The SimPowerSystem is used for this modeling work. The advantage of the SimPowerSystem is that it has extensive libraries for machines and power electronics circuits. In first section the Simulink model for the PMSM motor is given, in the next section the simulation results of DTC technique implemented with two level and three level inverter is given:

The motor parameters used for simulation are:

Stator resistance = 5.8  $\Omega$

Direct axis self inductance = 44.8 mH

Quadrature axis self inductance = 102.7mH

Rotor flux constant = 0.533 WB

Motor Moment of Inertia = .000329 kg-m<sup>2</sup>

Damping coefficient = .0003882 kg-m<sup>2</sup>/s

Number of poles = 2

## 5.2 MATLAB/Simulink model for PMSM :

The PMSM motor is modeled in MATLAB/Simulink using the modeling equations eqns 2.19 – 2.25 derived in chapter 2. The  $V_d$  and  $V_q$  voltages are obtained from the park's transformation of the stator abc voltages. The model is given below.

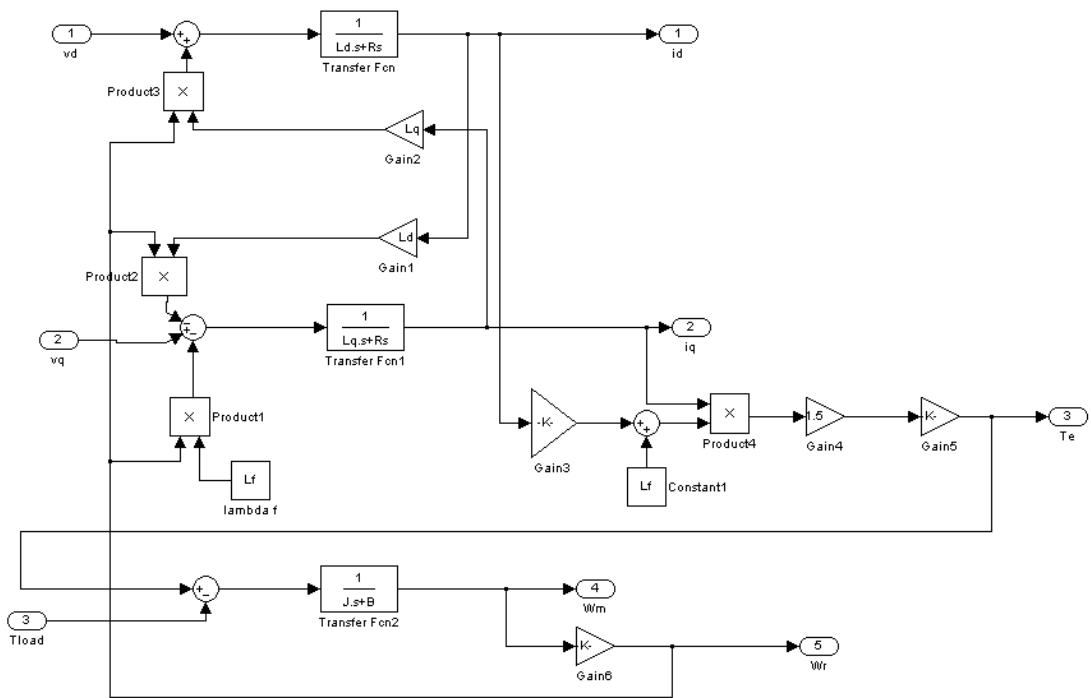


Figure 5.1. Simulink model of PMSM motor.

Park's transformation converts stator abc 3-phase voltages to equivalent 2-phase dq-reference frame ie, to the rotor reference frame. The eqns are given by eqn (2.11)

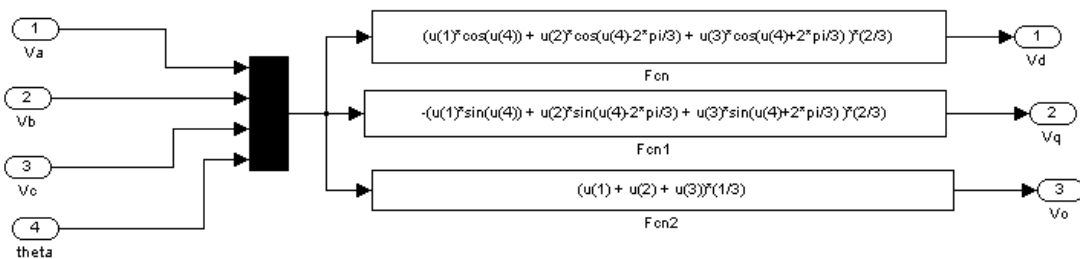


Figure 5.2. Park's Transformation block.

### 5.3 DTC TECHNIQUE WITH A TWO LEVEL INVERTER:

The control technique shown in fig 3.7 is implemented in MATLAB environment, and the simulink model is given below

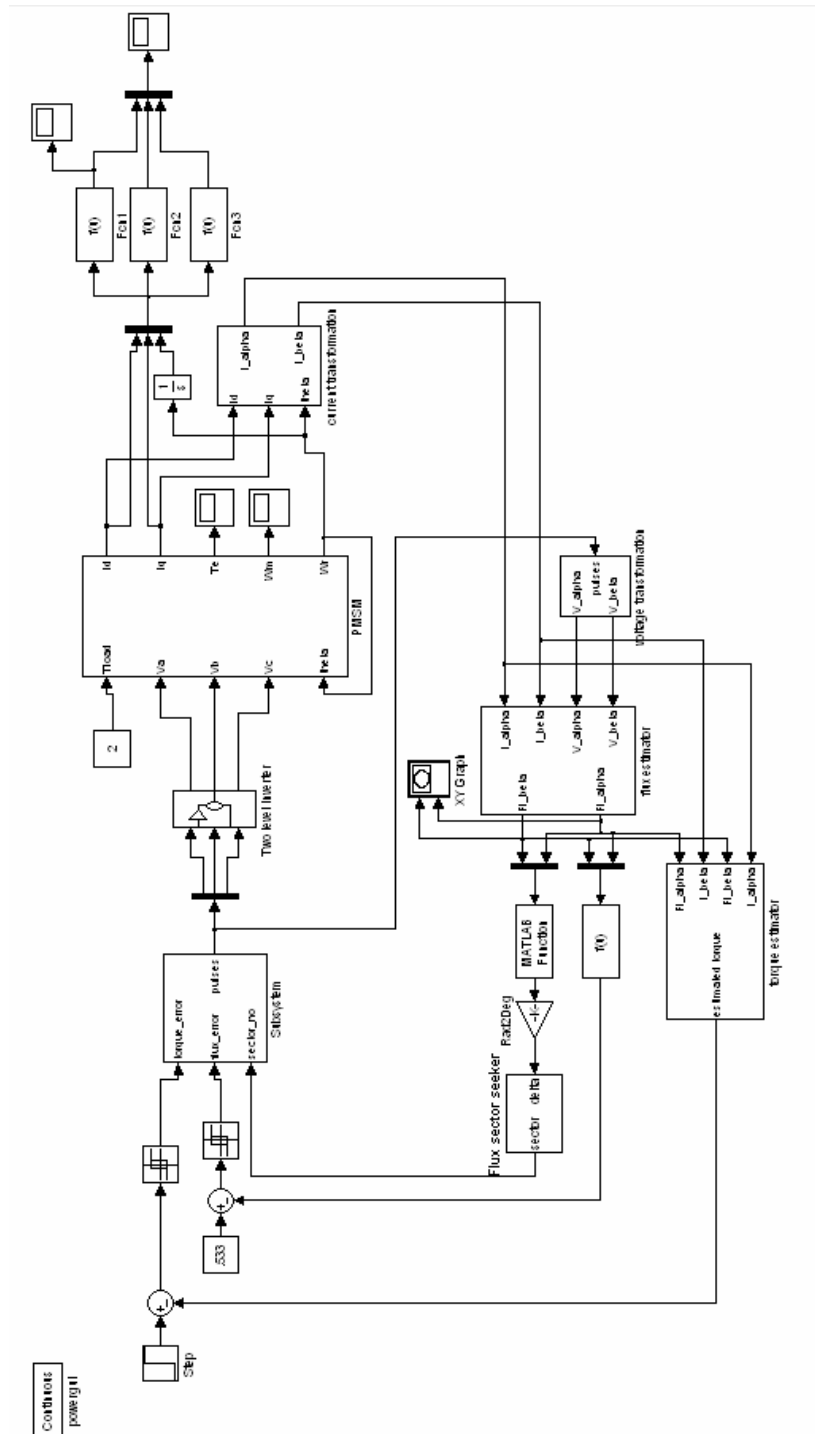


Figure 5.3. DTC with Two level inverter

With reference to the fig 5.3 the whole model can be divided into

PMSM motor model

Two level Inverter

Voltage vector selection table

Torque estimator and flux estimator

The torque and flux values are estimated from the eqns 3.18 and 3.19 and are compared with the reference values, the error is compared in hysteresis comparator and the output of the comparators along with the flux sector ( $\theta$ ) are together used in Switching table to determine the appropriate voltage vector. The vector selected from the Switching table is then applied to the Voltage Source Inverter (VSI). The voltages  $V_\alpha, V_\beta$  are estimated from the switching state of the each leg in the inverter.

The results for the above control technique are given below:

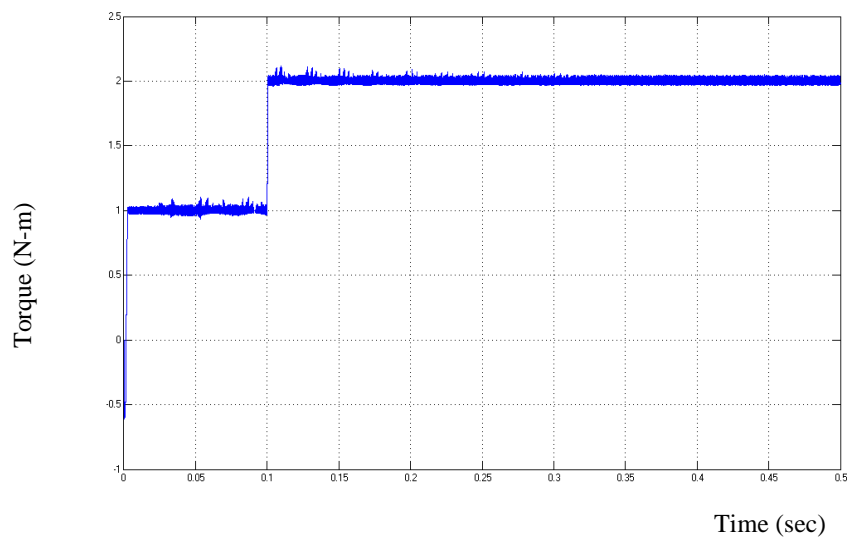


**Figure 5.4. Torque response of DTC with 2-level inverter.**

The command signal for the torque is taken as a step change changing from 1N-m to 2N-m at 0.1s. Fig 5.4 shows that the motor torque tracks the step change in command torque but with a large amount of ripple content.

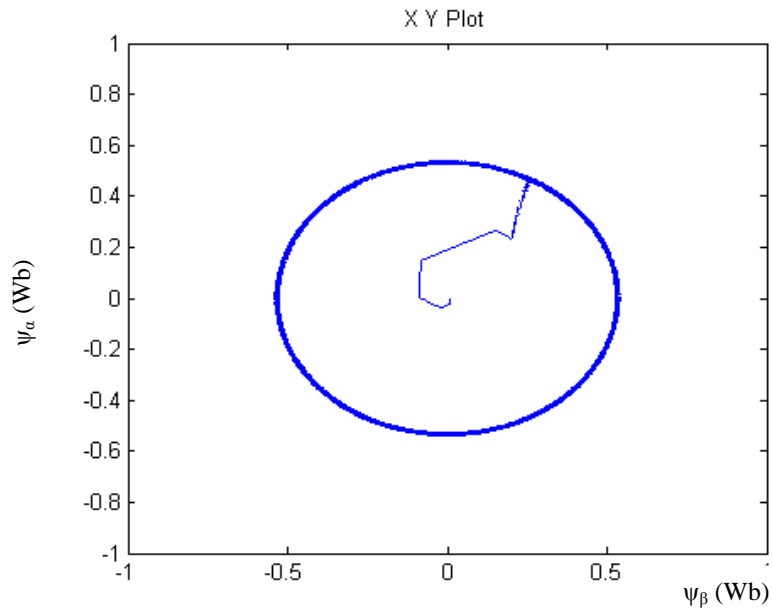


**Figure 5.5. Flux trajectory.**

A graph is drawn between the fluxes in  $\alpha\beta$ -axis i.e,  $\psi_\alpha$ , &  $\psi_\beta$ . The fig gives the locus of the flux vector in the  $\alpha\beta$ -plane which is a circle.

The steady state currents  $i_a$ ,  $i_b$  &  $i_c$  are shown in fig 5.6

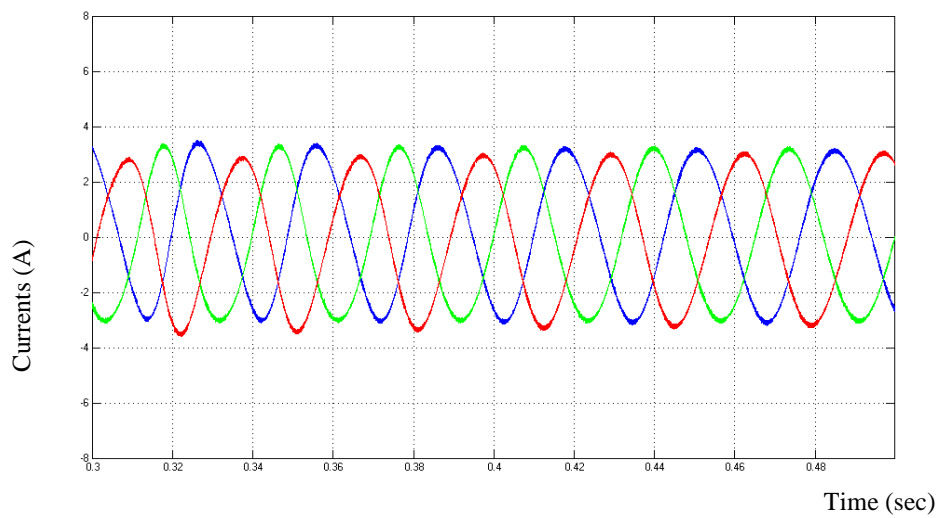


**Figure 5.6. Stator currents  $i_a$ ,  $i_b$  &  $i_c$ .**

The estimated stator flux is shown below. Fig 5.7 shows that the stator flux amplitude is restricted in a hysteresis width of .007.

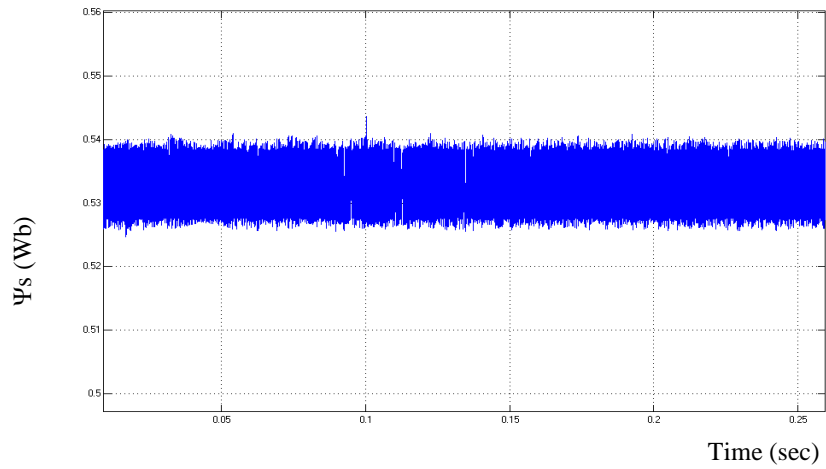


**Figure 5.7. Stator flux amplitude waveform.**

The spectrum for the stator current  $i_a$  is shown below. From the fig below it can be observed that the THD% in the current spectrum is about 29.67% and the fundamental component is .8495A.

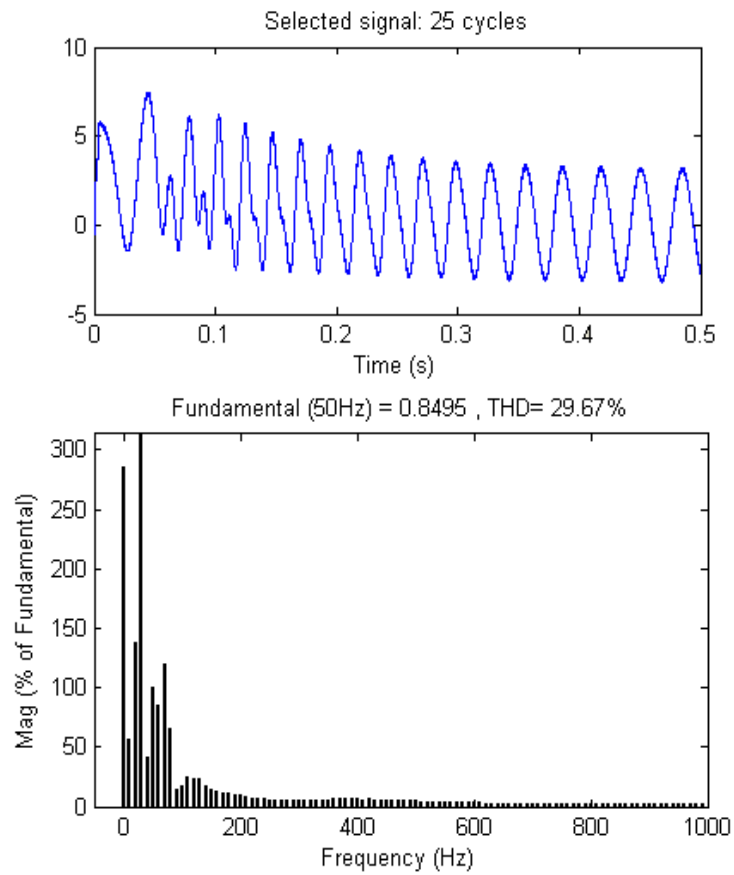


**Figure 5.8. Harmonic spectrum of Stator current.**

## 5.4 DTC TECHNIQUE WITH 3-LEVEL INVERTER:

The Direct Torque Control technique with 3-level inverter is implemented in MATLAB/Simulink and the results are shown. The drive parameters used for DTC with 2-level inverter are taken in 3-level inverter for comparison purpose. The results at each and every point is given below

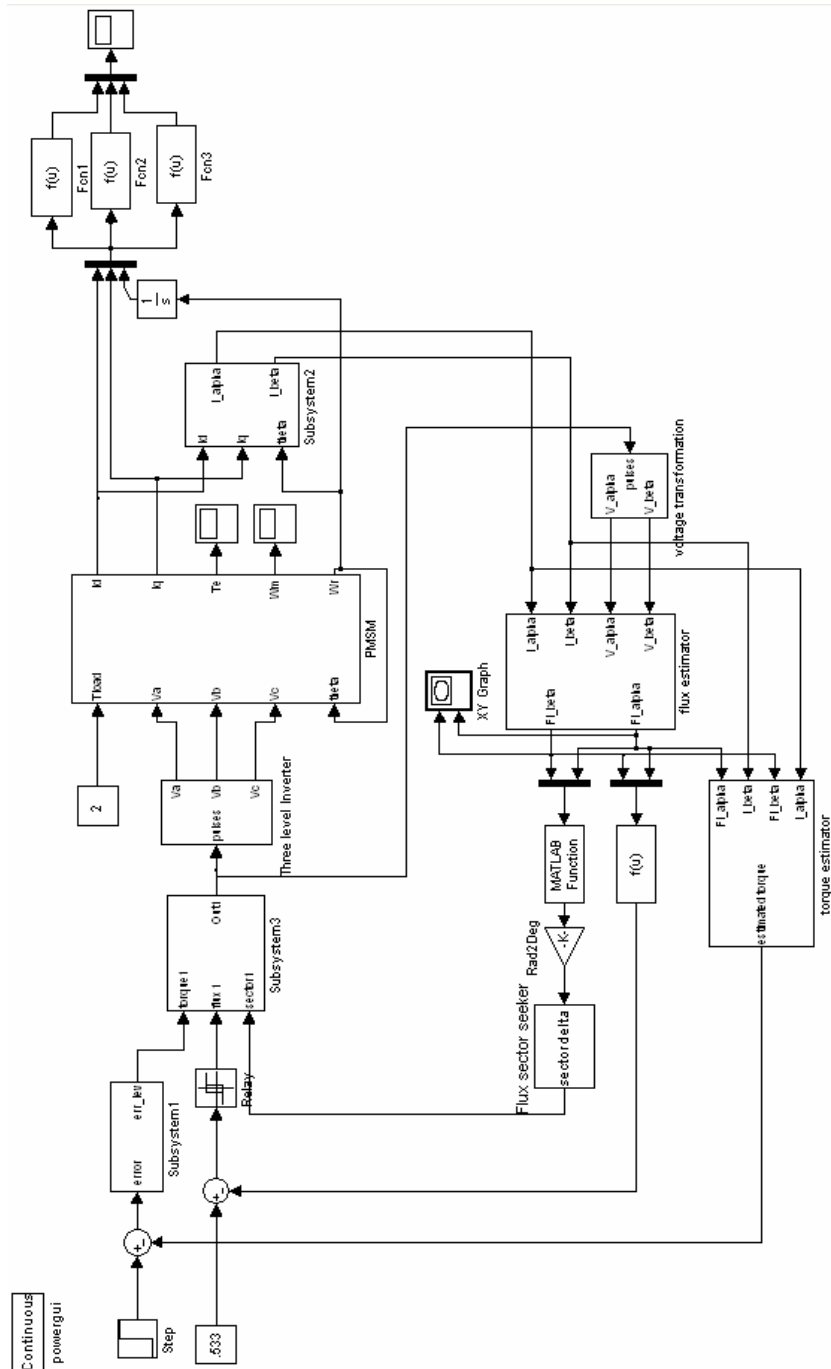
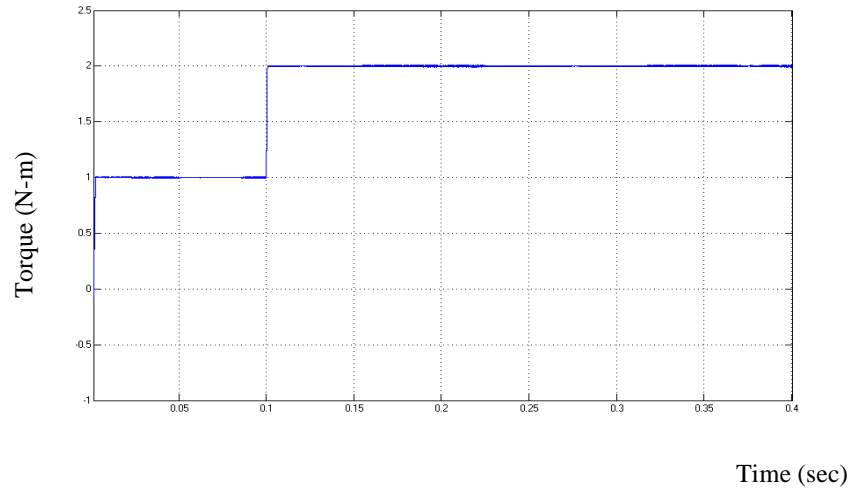


Figure 5.8. DTC with 3-level inverter.

The torque in 3-level inverter shown above contains less number of ripples as compared to DTC with 2-level inverter.



**Figure 5.9. Electro-magnetic torque with 3-level inverter.**

The plot between  $\psi_\alpha$  and  $\psi_\beta$  for DTC with a 3-level inverter is shown below

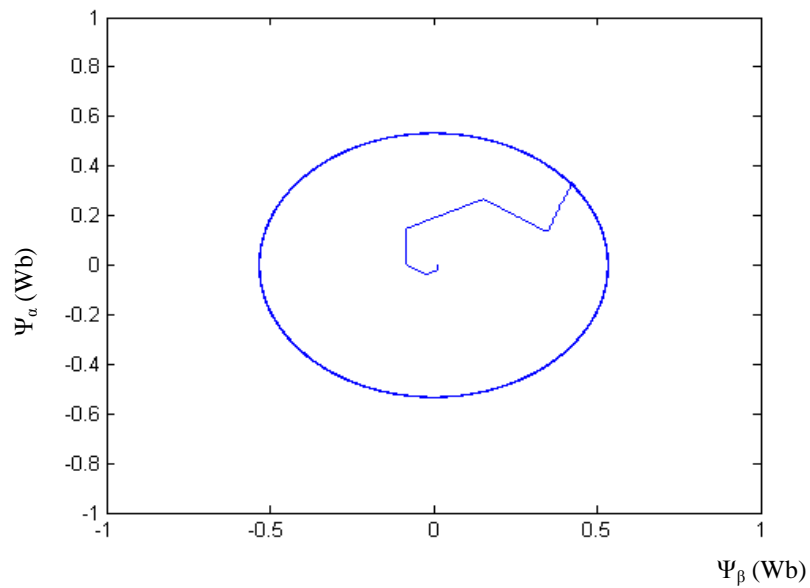


**Figure 5.10. Flux trajectory in 3-level inverter.**

The steady state stator currents  $i_a$ ,  $i_b$  &  $i_c$  are given below, which shows that the ripple in current is also reduced when compared to two level inverter

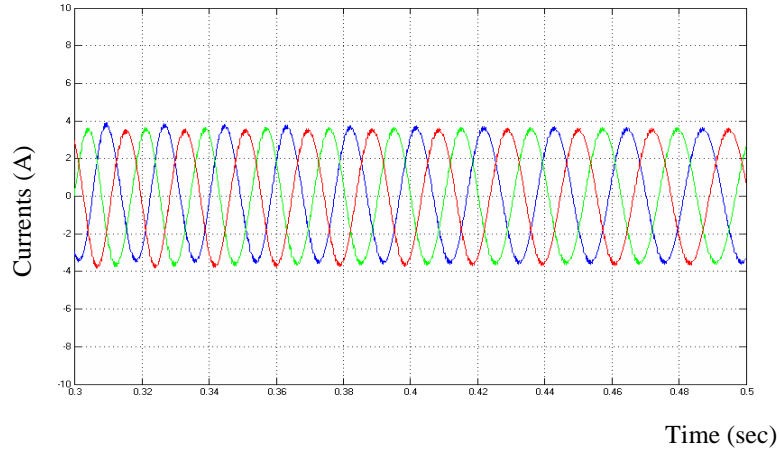


**Figure 5.11. Steady state Stator currents  $i_a, i_b$  &  $i_c$ .**

The estimated stator flux is shown in fig. 5.12. The result shows the ripples reduction when compared with two-level inverter.

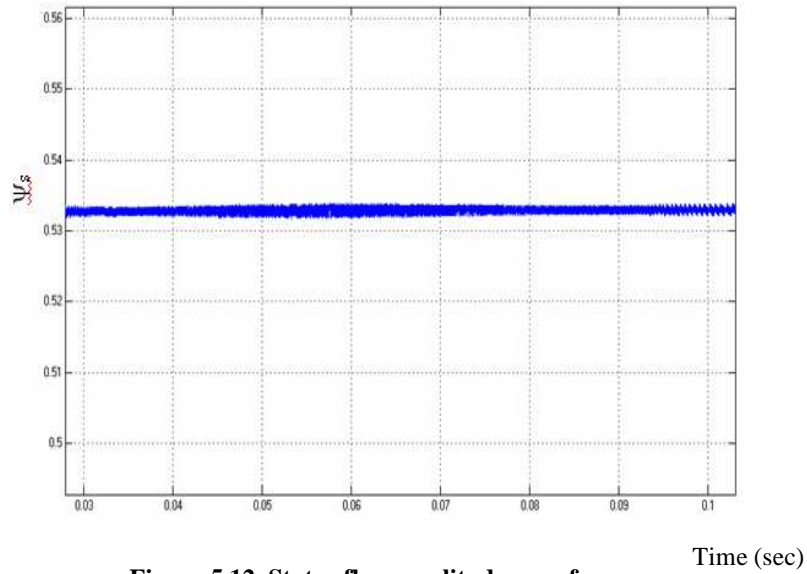


**Figure 5.12. Stator flux amplitude waveform.**

The stator current  $i_a$  spectrum for three level inverter is shown. The spectrum when compared with the spectrum of  $i_a$  with two level inverter the THD% has been reduced to 24.68 and also the fundamental component has been increased to 1.018A.

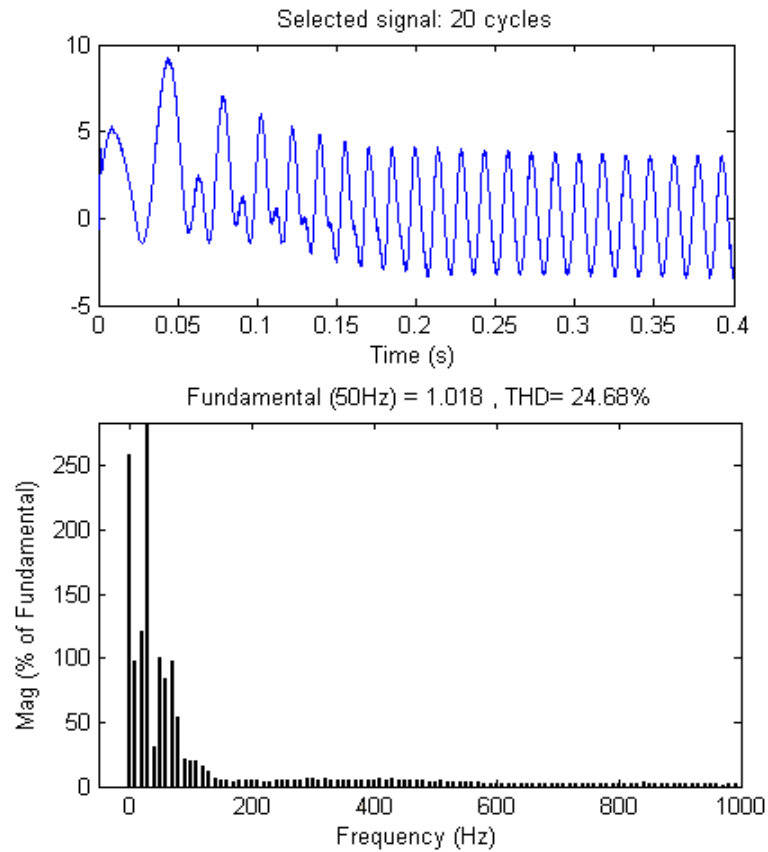


**Figure 5.13. Harmonic spectrum of Stator current.**

### 5.5 SUMMMARY:

In this chapter MATLAB Models and simulation results were presented. Matlab implementation Direct Torque Control Technique with both 2-level and 3-level inverter are done and results for both the cases are presented. Simulation results prove that the use of 3-level inverter instead of 2-level inverter in DTC technique results in lower ripple content in torque, stator flux and stator currents.

**TABLE 5.1 Comparison of PMSM with 2-level and 3-level inverter**

	Fundamental component of current	Percentage THD
With 2-level inverter	0.8495	29.67
With 3-level inverter	1.018	24.68

# **Chapter 6**

## **Conclusion and Recommendations**

## Chapter 6

### CONCLUSION AND RECOMMENDATIONS

Motor criteria such as durability, high performance, high power factor, easy and cheap control, low maintenance demands have led to a new type of motor excited by permanent magnets. In this thesis, by means of space vector theory, a mathematical model for the Permanent magnet Synchronous Motor is developed and implemented in MATLAB/Simulink

DTC is intended for an efficient control of the torque and flux without changing the motor parameters and load. Also the flux and torque can be directly controlled with the inverter voltage vector in DTC. Two independent hysteresis controllers are used in order to satisfy the limits of the flux and torque. In the performed simulation, certain stator flux and torque references are compared to the values estimated from the motor parameters and errors are sent to the hysteresis comparators. The outputs of the flux and torque comparators are used in order to determine the appropriate voltage vector and stator flux space vector.

In this thesis, DTC technique for a two level fed permanent magnet synchronous motor is explained and is simulated in MATLAB/Simulink environment. The simulation results are analysed and found that the torque obtained from the motor is having a large amount of ripple content. Therefore, in order to reduce the ripple content, the DTC technique is implemented with a three level inverter. In a three level inverter, the three levels in the phase voltage permit reduction of the harmonic content in stator voltages and currents and also in torque and flux ripples. The harmonic content in direct torque control technique for PMSM with a three level inverter can still be reduced by employing a new technique called DTC- Space Vector Modulation (DTC-SVM).

Direct Torque Control Technique of PMSM with a two level inverter can be implemented in Real-Time environment and the results can be validated with the obtained simulation results.

## **PAPERS FROM THESIS**

1. Paper Published entitled “Direct Torque Control of PMSM with a Two-Level Inverter using MATLAB/Simulink” in National conference on “**Recent Advances in Computational Techniques in Electrical Engineering**”, **Longowal**, Proceeding page number: 18, **Year-2010**.
2. Paper Published entitled “MATLAB/SIMULINK BASED DIRECT TORQUE CONTROL OF 3- $\Phi$  PMSM” in National conference on “**Recent Trends in Power Energy & Communication Engineering**”, **Puducherry**, Page number: 59-64, **Year-2010**.
3. Paper accepted for publication in “**International Journal of Engineering and Information Technology** “ (ISSN 0975-5292).

National Conference 2

Internation Journal 1

## **REFERENCES:**

- [1] M. Depenbrock, "Direct Self – Control (DSC) of Inverter Fed Induction Machine", *IEEE Trans. Power Electronics*, Vol. 3, No 4, October 1988.
- [2] Enrique L. Carrillo Arroyo "Modeling and Simulation of Permanent Magnet Synchronous Motor Drive system", Ph.D thesis, University of Puerto Rico Mayagüez campus, 2006.
- [3] Cui Bowen, Zhou Jihua, Ren Zhang, "Modeling and Simulation of Permanent Magnet Synchronous Motor Drive" *Fifth IEEE International Conference on Electrical Machines and Systems*, Volume 2, Aug. 2001.
- [4] Salih Baris Ozturk "Modelling, Simulation and Analysis of Low-cost Direct Torque Control of PMSM using HALL-EFFECT sensors", Ph.D thesis, Texas A&M University, December 2005
- [5] Pragasan Pillay, R. Krishnan "Modeling of Permanent Magnet Motor Drives", *IEEE Transactions on Industrial Electronics*, 1988.
- [6] S. Morimoto, Y. Tong, Y. Takeda, and T. Hirasu, "Loss minimization control of permanent magnet synchronous motor drives," *Industrial Electronics, IEEE Transactions on*, vol. 41, pp. 511-517, 1994.
- [7] L. Zhong, M. F. Rahman, "A Direct Torque Controller for Permanent Magnet Synchronous Motor Drives", *IEEE Trans. On Energy Conversion*, Vol. 14, No.3, September, 1999.
- [8] S. Dan, F. Weizhong, H. Yikang, "Study on the Direct Torque Control of

Permanent-Magnet Synchronous Motor Drives", *Fourth IEEE International Conference on Power electronics and Drive System*, October 22-25, Bali, Indonesia, p. 571-574.

- [9] L. Zhong, M. F. Rahman, W.Y. Hu, K.W. Lim, "Analysis of Direct Torque Control in Permanent Magnet Synchronous Motor Drive", *IEEE Trans. On Power Electronics*, Vol. 12, No.3, May, 1997.
- [10] Sariati Binti Dalib," The Simulation of the Direct Torque Control of Permanent Magnet Synchronous Motor"University Technology, Malaysia, May, 2007.
- [11] D.Casadei, Francesco Profumo, Giovanni Serra, Angelo Tanni, "FOC and DTC: two viable schemes for Induction Motor Torque control", *IEEE transactions on Power Electronics*. 2002.
- [12] LANG Bao-hua, LIU Wei-guo, ZHOU Xi-wei, LI Rong, "Research on Direct Torque Control of Permanent Magnet Synchronous Motor Based on Optimized State Selector", *IEEE ISIE Volume 3*, 9-13 July 2006.
- [13] Rahman MF, Zhong L. "Voltage switching tables for DTC controlled interior permanent magnet motor", *IECON'99, 25th annual Conference* June, 1999. p. 1445-51.
- [14] Maurizio Cirrincione , Marcello Pucci, Gianpaolo Vitale "A Novel Direct Torque Control of an Induction Motor Drive with a Three-Level Inverter", *IEEE Bologna PowerTech Conference*, June 23-:26.2003.
- [15] K. E. B. Quinderé, E. Ruppert F., Milton E. de Oliveira F, "Direct torque control of permanent magnet synchronous motor drive with a three-level

inverter” *IEEE Trans. On Power Electronics*, 18-22 June 2006.

- [16] D.Casadei, Giovanni Serra, Angelo Tanni “Improvement of Direct Torque Control by using a discrete SVM technique”, *IEEE transactions on Power Electronics*.1998.
- [17] David Ocen “Direct Torque Control of a Permanent Magnet synchronous Motor” Ph.D thesis, Stockholm, Sweden 2005.
- [18] Jurgen K. Steinke “Control strategy for three phase AC traction Drive with Three-level GTO-PWM inverter”, *PESC*.1988.
- [19] Thomas G. Habetler and Deepakraj M. Divan “Control strategies for Direct Torque Control using Discrete Pulse Modulation”, *IEEE transactions on Industrial applications*, VOL.27 page(s). 893-901.1991.
- [20] Chapuis, Y.A.; Roye, D.; Davoine, J “Principles and implementation of direct torque control by stator flux orientation of an induction motor”, *Applied Power Electronics conference proceedings*, vol.1 Page(s):185 – 191. 1995.
- [21] Xavier del Toro Garcia, Antoni Arias, Marcel G. Jayne, Phil A. Witting, Vicenç M. Sala, Jose Luis Romeral “New DTC Control Scheme for Induction Motors fed with a Three-level Inverter”, *AUTOMATIKA*, Pages 73–81.2005.